

Kinematic Analysis and Metamorphic Character  
Of A Shear Zone In The Thelon Front,  
Artillery Lake Area, District of  
Mackenzie, N.W.T.

KINEMATIC ANALYSIS AND METAMORPHIC  
CHARACTER OF A SHEAR ZONE IN THE  
THELON FRONT, ARTILLERY LAKE AREA  
DISTRICT OF MACKENZIE, N.W.T.

by

STUART MALCOLM MILLER

A Thesis

Submitted to the Department of Geology  
in Partial Fullfillment of the Requirements for the  
Degree Honours Bachelor of Science

McMaster University

April, 1987

BACHELOR OF SCIENCE (HONOURS), (1987) McMaster University,  
(Geology) Hamilton, Ontario

TITLE: Kinematic Analysis And Metamorphic  
Character Of A Shear Zone In The Thelon  
Front, Artillery Lake Area, District of  
Mackenzie, N.W.T.

AUTHOR: Stuart Malcolm Miller

SUPERVISOR: Dr. P. M. Clifford

NUMBER OF PAGES vii, 91

## Abstract

The Artillery Lake area is diagonally bisected by the north-northeasterly trending Thelon Front. The best single surface feature to represent the Thelon Front is the "straight zone" which is a zone of porphyroclastic metasediments that also contains the study area. Kinematic indicators observed in the study area include extensional shear surfaces, C&S fabric, mica "fish", asymmetrical porphyroclast tails, asymmetrical folds, microfaulted porphyroclasts and secondary quartz subgrain foliations. Kinematic analysis of these features has shown that right lateral simple shear displacements and "east-side-up" vertical shear displacements have been accommodated within the rocks of the study area. The displacement senses determined by kinematic analysis are consistent with the regional data indicating progressively deeper exposures of structural levels to the east which suggests vertical motions localized at the domain boundaries. The stretching lineation present in the area is a combination of passive and direct extensions due to sub-vertical motions in the shear zone. A transition from early-ductile to late-brittle feldspar deformation textures indicates that metamorphic conditions during initial deformation were at epidote-amphibolite facies and relaxed during the later stages of deformation to greenschist facies.



## Acknowledgements

I would like to thank Dr. P.M. Clifford for his helpful insites, advise and direction in the completion of this thesis of which he originally knew nothing about and Dr. R.H. McNutt for his critical review of the final draft.

I am indebted to Dr. John B. Henderson of the Geological Survey of Canada for the oppourtunity to undertake this project and, along with the rest of the Smart Lake crew (Otto van Breeman, Jerry Dionne, Melanie Haggart, Don James, Rob and Martha McFie, Peter McGrath, Owen Steele, Rick Welther, and Natasha Wodica) whose good company made for a great field season.

Jack Whorwood's expert photography, Len Zwicker's professionally prepared thin sections and Trudy Chin's speedy typing and great patience contributed to the completion and quality of this thesis. I would also like to thank my officemates in room 130 for their good company, informative discussions and generosity with their drafting equipment. Lastly I would like to thank the rest of the fourth year graduatig class for making these last couple years the best times of my life.

## Table Of Contents

|   |     |
|---|-----|
| <b>Abstract</b>   | iii |
| <b>Acknowledgements</b>   | iv  |
| <b>Table of Contents</b>  | v   |
| <b>List of Figures</b>  | vi  |
| <b>List of Tables</b>   | vii |
| <b>Chapter 1: Introduction</b>  |     |
| Geographic Location, Access<br>and Purpose  | 1   |
| Previous Work and Regional Geology  | 1   |
| General Structural Divisions  | 7   |
| Metamorphism  | 10  |
| <b>Chapter 2: Petrography</b>   |     |
| Unit Description  | 12  |
| Thin Section Petrography  | 15  |
| Discussion of Petrography   | 19  |
| <b>Chapter 3: Kinematics</b>  |     |
| Introduction  | 23  |
| Mesoscopic Structures   | 25  |
| Microscopic Structures  | 42  |
| <b>Chapter 4: Discussion</b>  |     |
| Introduction  | 65  |
| Stain Estimate  | 66  |
| Mesostructures and Microstructures:<br>Foliation and Lineation                            | 67  |
| Feldspar Porphyroclasts   | 68  |
| Extensional Shear Surfaces and<br>Mica "Fish"   | 74  |
| Asymmetrical Folds  | 76  |
| Secondary Quartz Subgrain Foliations  | 78  |
| Discussion of Metamorphism, Micro-<br>structures, Mesostructures and<br>"The Big Picture" | 80  |
| <b>Chapter 5: Conclusions</b>   |     |
| Conclusions   | 84  |
| Suggestions for Further Research  | 85  |
| <b>References</b>   | 86  |



## List Of Figures

| <u>Figure</u>  | <u>Page</u> |
|--|-------------|
| 1. Generalized geology of the Artillery Lake area . . .              | 5           |
| Legend to Figure 1. . . . .  | 6           |
| 2. Finely laminated mylonite . . . . .                               | 13          |
| 3. Coarse-grained porphyroclasts . . . . .                           | 13          |
| 4. Map of study area . . . . .                                       | 27          |
| 5. Stereoplot of structural data . . . . .                           | 29          |
| 6. Corrugation lineation . . . . .                                   | 31          |
| 7. C-surface . . . . .   | 32          |
| 8a. Symmetrical pull aparts . . . . .                                | 35          |
| 8b. Asymmetrical pull aparts . . . . .                               | 35          |
| 9a. Asymmetrical porphyroclast tails . . . . .                       | 36          |
| 9b. Porphyroclast aligned along fold limb . . . . .                  | 36          |
| 10. Cartoon of stretched quartz-feldspar layers . . . . .            | 37          |
| 11a. Open folds . . . . .  | 39          |
| 11b. Tight folds . . . . .   | 39          |
| 12a. Kink band . . . . .   | 41          |
| 12b. Sinistral fault . . . . .                                       | 41          |
| 13a. C-surfaces . . . . .  | 44          |
| 13b. C&S Fabric . . . . .  | 44          |
| 14. Mica "fish" . . . . .  | 46          |
| 15. Asymmetrical microfold . . . . .                                 | 46          |
| 16a. Feldspar pull apart . . . . .                                   | 50          |
| 16b. Feldspar pull apart . . . . .                                   | 50          |
| 17a. Sympathetically fractured porphyroclast . . . . .               | 52          |
| 17b. Antithetically fractured porphyroclast . . . . .                | 52          |
| 18. Brittle-ductile deformation in porphyroclast . . . . .           | 54          |
| 19. Undulatory extinction in porphyroclast . . . . .                 | 54          |
| 20a. Sigmoidal twins in porphyroclast . . . . .                      | 56          |
| 20b. Kink band in porphyroclast . . . . .                            | 56          |
| 21. Asymmetrical porphyroclast tails . . . . .                       | 58          |
| 22a. Subgrain foliation in quartz ribbon (prep. $L_S$ ) . . . . .    | 61          |
| 22b. Subgrain foliation in quartz vein (perp. $L_S$ ) . . . . .      | 61          |
| 23a. Subgrain foliation in quartz ribbon (parallel $L_S$ ) . . . . . | 62          |
| 23b. Subgrain foliation in quartz vein (parallel $L_S$ ) . . . . .   | 62          |
| 24. Axial planar-parallel subgrain foliation . . . . .               | 64          |
| 25a. Porphyroclast textures . . . . .                                | 71          |
| 25b. Strain ellipsoid . . . . .                                      | 71          |
| 26. Stereoplot with strain axes positions . . . . .                  | 81          |

List Of Tables

| <u>Table</u> |  | <u>Page</u> |
|--------------|--|-------------|
| 1.           | Minerals characterizing metamorphic facies . . . . . | 20          |
| 2.           | Structural data . . . . .                            | 28          |
| 3.           | Microfabrics observed in thin sections . . . . .     | 48          |



## Chapter 1: Introduction

### Geographic Location, Access and Purpose

The study area is located within the Artillery Lake map area which is approximately 400 kilometers east of Yellowknife in the District of Mackenzie, Northwest Territories. Access is by aircraft only from Yellowknife to Smart Lake located at  $106^{\circ} 45' 55''$  longitude and  $63^{\circ} 30' 50''$  north latitude. The small island off the south shore of the northeast arm of Smart Lake is the study area (Figure 1).

The primary purpose of this work is to characterise the deformation of the rocks in the immediate study area, as well as their metamorphic character. This study may contribute information as to the nature and style of deformation in the Artillery Lake area and so shed further light on the nature of the Thelon Front.

### Previous Work and Regional Geology

The Thelon Front was originally recognised during 1:1,000,000 scale regional helicopter reconnaissance mapping of the northwestern Shield as part of Operation Thelon (Wright, 1957, 1967; Fraser, 1964). It has recently been the

focus of more detailed studies being carried out by various officers of the Geological Survey of Canada in its northern (Thompson et al., 1986), central (Frith, 1982; Henderson et al., 1982, 1987; Henderson and Thompson, 1980, 1982) and southern (Bostock, 1987) sections, all part of an ongoing program to examine the nature and significance of the Thelon Front.

The Artillery Lake area which straddles the Thelon Front was originally mapped during Operation Thelon (Wright, 1957). More detailed work continued on the area in succeeding years (Wright, 1967; Fraser, 1972) culminating in the project recently completed during the 1986 field season by Henderson et al. (1987) during which field work for this study was completed. The completion of this project also involved geophysical studies incorporating magnetic and VLF ground geophysical surveys as well as a series of gravity profiles across the area (Henderson et al., 1987; McGrath and Henderson, 1985).

A more detailed 1:50,000 scale structural and metamorphic study is currently underway by James (1986) on the central part of the Thelon Tectonic Zone near Moraine Lake as well as other detailed structural (eg. Hanmer and Lucas, 1985), metamorphic (Hanmer and Connelly, 1986), geochronological (van Breeman et al., 1987), and sedimentological (Grotzinger et al., 1986) studies in other sections of the Thelon Front. McFie (1987) undertook



detailed mapping of an anorthosite body adjacent to Clinton-Colden Lake as a Masters thesis and Ghandi (1985) recently completed studies of the geology and mineral deposits in the southwest part of the area at Artillery Lake.

The Artillery Lake map area is diagonally bisected by the north-northeasterly trending Thelon Front. This structural and metamorphic discontinuity separates the Slave Province from the Thelon Tectonic Zone of the Churchill Province. The former is characterized by curvilinear structural trends, massive plutonic bodies and low to intermediate grade supracrustal rocks of the Yellowknife Supergroup while the latter is characterized by linear structural trends, strongly foliated plutons and gneisses and foliated schists of high metamorphic grade. The area has been recognized as containing 4 domains, differentiated from one another by litho-structural variations (Figure 1). Progressively deeper exposures of structural levels are implied by a general increase in deformation and metamorphic grade from west to east.

The western domain contains metasedimentary, metavolcanic and intrusive igneous rocks typical of the Slave Province. The metasediments are thought to represent the mudstone-graywacke turbidites of the Yellowknife Supergroup; the metavolcanics, also of the Yellowknife Supergroup, are presumed to be related to the major mafic volcanic complex east of Clinton-Colden Lake. Archean ages have been deter-

mined for these rocks (Henderson, 1970, 1985). Penetrating these supracrustal rocks are granitoid rocks of both gneissic and massive character. These, too, are Archean in age but have been affected by post-Archean metamorphic events. A unit of early Paleozoic carbonates outcrops on the southeast shore of Artillery Lake; these rocks show an unconformable, lower fault contact with the adjacent Archean rocks.

The central domain, being transitional between the eastern and western domains, shows characteristics of both. Migmatitic equivalents of the Yellowknife metasediments are present in this domain and the major belt of Yellowknife supracrustals at the eastern boundary of the domain contains the "straight zone", a portion of which is focus of this study. The gneissic and granitic to granodioritic intrusive phases of this domain are generally well foliated.

The eastern domain, part of the Thelon Tectonic Zone, contains rocks that are the most deformed, of the highest metamorphic grade and the most lithologically distinctive of the northern domains. This domain shows the most complex litho-structural relationships in the map area and dating of various units has yielded dates of granulite grade metamorphism and younger intrusive phases (van Breeman, 1987).

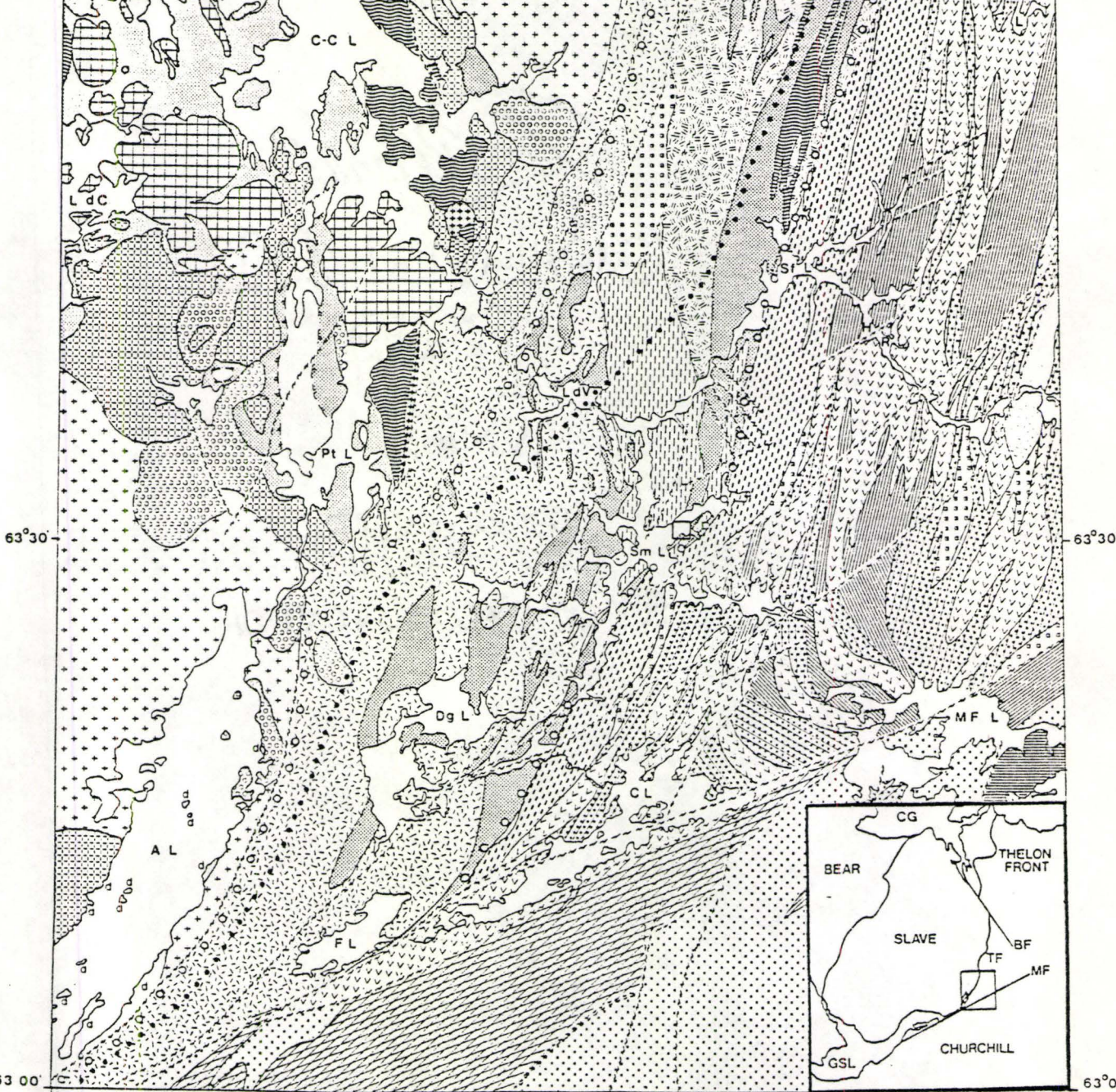
The southern domain contains rocks of an exotic terrain that has been translated into the area along the McDonald Fault from an area approximately 70 kilometers to the east as



Figure 1. Generalized geology of the Artillery Lake area (from Henderson et al., 1987). Study area indicated by small square. Inset showing the Artillery Lake area; GSL-Great Slave Lake, CG-Coronation Gulf, TF-Thelon Front, BF-Bathurst Fault, MF-McDonald Fault.



64°00' 108°00' 107°00' 106°00' 64°00'

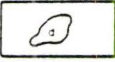
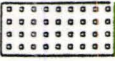
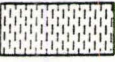

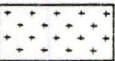

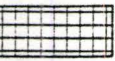
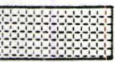

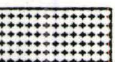






63°00' 108°00' 107°00' 106°00' 63°00'



# Legend to Figure 1.

## WESTERN AND CENTRAL DOMAINS

-  DOLOMITE, ARTILLERY LAKE FORMATION, EARLY PROTEROZOIC
-  GRANODIORITE, GRANITE, PINK AND BLACK, MEGACRYSTIC, BIOTITE, MODERATELY TO STRONGLY FOLIATED
-  GRANITOID MIGMATITE; PINK AND GREY, BIOTITE-HORNBLLENDE, MODERATELY FOLIATED
-  FOLIATED GRANITOIDS TO GRANITIC GNEISSES UNDIVIDED;
-  GRANITE, GRANODIORITE; BIOTITE (MUSCOVITE) MEGACRYSTIC, MASSIVE
-  GRANITE; BIOTITE- MUSCOVITE, MASSIVE
-  GRANODIORITE; BIOTITE (HORNBLLENDE), MASSIVE
-  TONALITE, DIORITE; HORNBLLENDE-BIOTITE, MASSIVE
-  QUARTZ DIORITE, DIORITE;
-  ANORTHOSITIC GABBRO, ANORTHOSITE
- YELLOWKNIFE SUPERGROUP**
-  METAGREYWACKE, PELITE AND HIGH GRADE EQUIVALENTS; (A) GREENSCHIST FACIES (B) AMPHIBOLITE FACIES (C) MIGMATITE
-  MAFIC TO INTERMEDIATE METAVOLCANIC ROCKS GREENSCHIST TO AMPHIBOLITE GRADE
-  GRANITOID GNEISSES; HETEROGENEOUS COMPOSITION, RECRYSTALLIZED IN PART, IN PART POSSIBLY OLDER THAN YELLOWKNIFE

 Study Area

 GEOLOGICAL CONTACT; DEFINED OR ASSUMED

 FAULT, SHEAR ZONE

 METAMORPHIC ISOGRAD


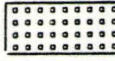


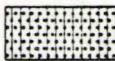

 DOMAIN BOUNDARIES

 LINE OF INFLECTION BETWEEN POSITIVE AND NEGATIVE REGIONAL PAIRED GRAVITY ANOMALY







KILOMETERS

## EASTERN DOMAIN

-  GRANITE, GRANODIORITE; BIOTITE, STRONGLY FOLIATED
-  GRANODIORITE, GRANITE; PINK AND BLACK, MEGACRYSTIC, BIOTITE, MODERATELY TO STRONGLY FOLIATED
-  GRANITOID MIGMATITE; BIOTITE-HORNBLLENDE, PINK AND GREY, STRONGLY FOLIATED
-  GRANITOID GNEISSES TO FOLIATED GRANITOIDS UNDIVIDED, SOME SUPRACRUSTAL GNEISSES
-  MIGMATITIC METASEDIMENTARY GNEISSES; WITH YOUNGER GRANITIC SHEETS AND INTRUSIONS
-  MIGMATITIC AMPHIBOLITE TO QUARTZOFELDSPATHIC AMPHIBOLE BEARING SUPRACRUSTAL GNEISS; WITH GRANITIC SHEETS AND INTRUSIONS

## SOUTHERN DOMAIN

-  GRANODIORITE, GRANITE; BIOTITE, MEGACRYSTIC TO PORPHYROCLASTIC, FOLIATED
-  GRANITOID GNEISSES TO FOLIATED GRANITOIDS UNDIVIDED, SOME SUPRACRUSTAL GNEISSES
-  MIGMATITIC METASEDIMENTARY GNEISSES; WITH YOUNGER GRANITIC SHEETS AND INTRUSIONS
-  MIGMATITIC AMPHIBOLITE TO AMPHIBOLITIC GNEISS; WITH GRANITIC SHEETS AND INTRUSIONS

## LAKE SYMBOLS

- A L ARTILLERY LAKE
- C L CAMPBELL LAKE
- C-C L CLINTON-COLDEN LAKE
- DG L DOUGLAS LAKE
- F L FORD LAKE
- H R HANBURY RIVER
- L DC LAC DE CHARLOIT
- L DV LAC DEVILLE
- M L MORaine LAKE
- M F L MARY FRANCES LAKE
- Pt L PTARMIGAN LAKE
- SF L SIFTON LAKE
- SM L SMART LAKE
- W L WILLIAMS LAKE

interpreted from aeromagnetic anomaly reconstruction (Thomas et al., 1976; Henderson et al., 1987).

In addition to the many gneissic and intrusive rocks mentioned above, the area also contains several sets of post Archean diabase dykes and a set of younger north-northwesterly trending dykes.

The Artillery Lake area therefore shows a transition from the Slave Province in the west to the Thelon Tectonic Zone in the east as well as a displaced terrain of the Central Thelon Tectonic Zone. Although many detailed and regional studies have contributed much data towards the understanding of the Thelon Front, the precise nature and tectonic significance of this major structural and metamorphic discontinuity is still the subject of continuing debate.

### General Structural Divisions

The Artillery Lake map area has been subdivided into four major structural domains on the basis of structural trends as well as relative degree of deformation and lithology. The boundaries themselves are defined by north-northeasterly trending faults or shear zones, and by the northeasterly trending McDonald Fault in the case of the boundary separating the southern domain from the east and central domains.



In the western domain structural trends of foliations and gneissosity are generally northerly to northwesterly but locally they conform to the outline of the intrusions; dips are generally steep. The foliation and gneissosity of the central domain have a northerly strike with local variations and are also steeply dipping while the rocks of the eastern domain have a very pronounced north-northeasterly trending foliation or gneissosity with dips steeply to the east particularly in the northwestern part of the domain. The trends in the southeast portion of the domain become more varied and generally more moderately dipping, even flat in some areas. The eastern domain also contains a series of subdomains bounded by shear zones that are either lithological or geophysical breaks (Henderson et al., 1987). The southern domain truncates the other three domains and differs markedly in structural style from the adjacent eastern domain. Structural trends of the units in this domain are generally northeasterly but show highly variable trends in detail. Zones of mylonite to ultramylonite occur at some unit contacts and within units, some showing northeasterly trends.

The major structures in the map area include the "straight zone", a zone of porphyroclastic metasediments and two sets of faults.

The "straight zone" is thought to be the best single feature to represent the Thelon Front in the northern part of the Artillery Lake area and in the Healey Lake sheet to the

north but the straight zone thins significantly to the south and changes its trend through part of Smart Lake (Henderson et al., 1982). In this bend in the straight zone there is a small island with excellent exposure and easy access; this was chosen as the study location.

The locus of inflection of a large paired gravity anomaly passes through the Artillery Lake area, closely following the "straight zone" suggesting a relationship between these two features. This anomaly is thought to represent a major, deep crustal contact, probably the deep trace of the Thelon Front (Henderson et al., 1987). The locus of inflection deflects to a position southwest of the straight zone south of Sifton Lake (Figure 1). If the straight zone is considered to be the surface expression of the Thelon Front to the north of Sifton Lake, then this suggests the straight zone becomes less important as an expression of the Thelon Front in the southern portion of the map area. A complete understanding of these trends and their relationship to the Thelon Front depends upon more comprehensive interpretations of the data available.

Of the two fault sets in the Artillery Lake area one trends northeasterly and is associated with the McDonald fault. The other set trends north-northwesterly, and is associated with the Bathurst Fault which "offsets" a major part of the Thelon Tectonic Zone to the north of the Healey Lake area, one sheet north of the Artillery Lake map area.

The McDonald Fault itself shows significant dextral displacement and also displays evidence of a significant vertical component in the form of a southwesterly plunging stretching lineation in ductile zones. The other fault set associated with the Bathurst Fault shows a sinistral sense of displacement. This fault set also displays ductile characteristics in some localities.

Many of the structural features of the regional geology are also expressed in the rocks of the study area and this will permit some comparisons between local and regional characteristics.

### Metamorphism

The metamorphic character of the Artillery Lake map area is dominated by an increase in metamorphic grade along a west to east transect which has been interpreted as reflecting exposures of progressively deeper structural levels (Henderson and McFie, 1986).

The western domain contains rocks of the dominantly low grade greenschist Yellowknife Supergroup and shows locally steep metamorphic gradients (Henderson et al., 1987), a pattern which is similar to the pattern displayed by the rocks of the central Slave Province. This contrasts strongly with the high grade migmatites which are thought to be

Yellowknife equivalents in the central domain. This domain also contains a zone of high pressure metamorphism indicated by the presence of kyanite in a belt of Yellowknife metasediments east of the straight zone but this high pressure zone does not appear to extend south of Sifton Lake (Figure 1).

The eastern domain contains a zone of granulite grade rocks whose western boundary is sharply defined and is parallel to the domain boundary. The zone itself is up to 10 km wide and corresponds approximately to a north-northeasterly trending positive gravity anomaly, but the eastern boundary of the zone of granulite grade rocks is poorly defined, trending into sporadic zones within the upper amphibolite rocks that underlie much of the rest of the domain.

The southern domain contains amphibolitic to migmatitic high grade rocks as well as biotite-garnet-rich supracrustal gneisses similar to the granulite grade supracrustal gneisses of the eastern domain. The McDonald Fault defines a metamorphic break between the three northern domains and the southern domain.

A more detailed discussion of metamorphism is undertaken in chapter 4.



## Chapter 2: Petrography

### Unit Description

There is really only one rock unit in the study area. This unit is a generally fine grained, dark to light gray, porphyroclastic mylonite that is the highly deformed equivalent of a migmatized metasediment of the Yellowknife Supergroup. The unit shows some variation in composition at outcrop scale expressed as contrasts in mica (biotite + muscovite) content of the rock. These variations are probably inherited from heterogeneities in the distribution of the mica-rich paleosome and the quartz/feldspar-rich leucosome evident in the much less deformed parent migmatite elsewhere in the Artillery Lake map area.

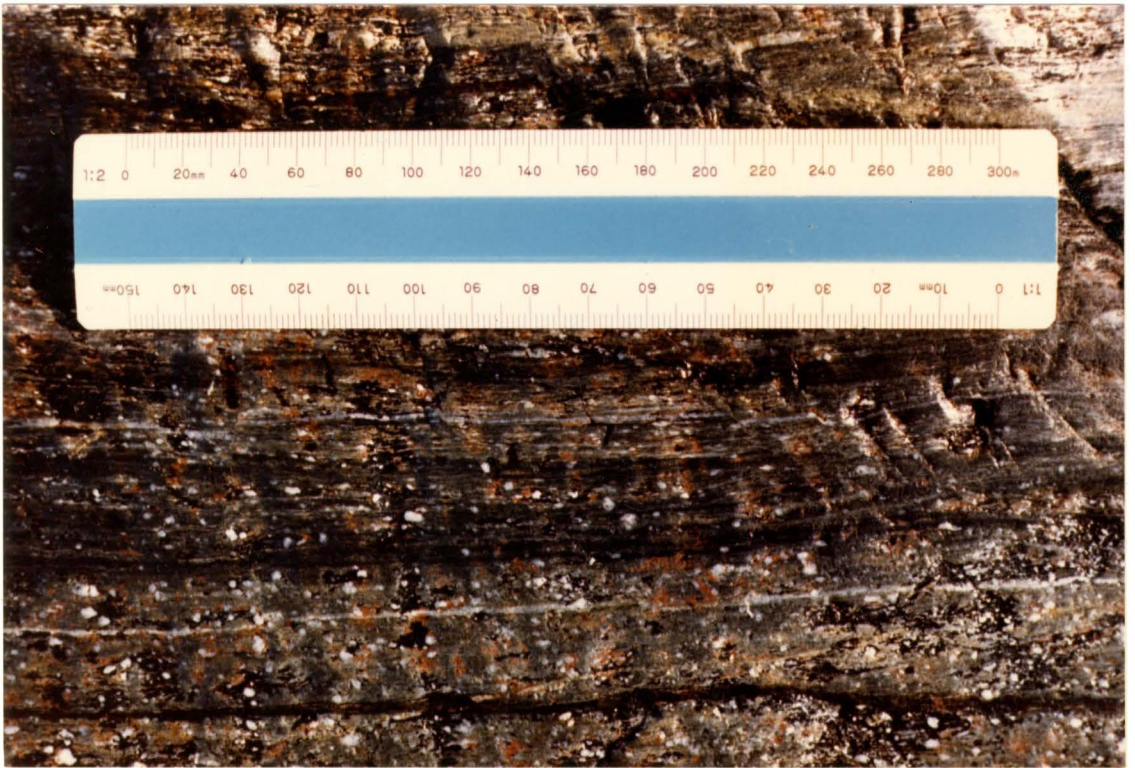
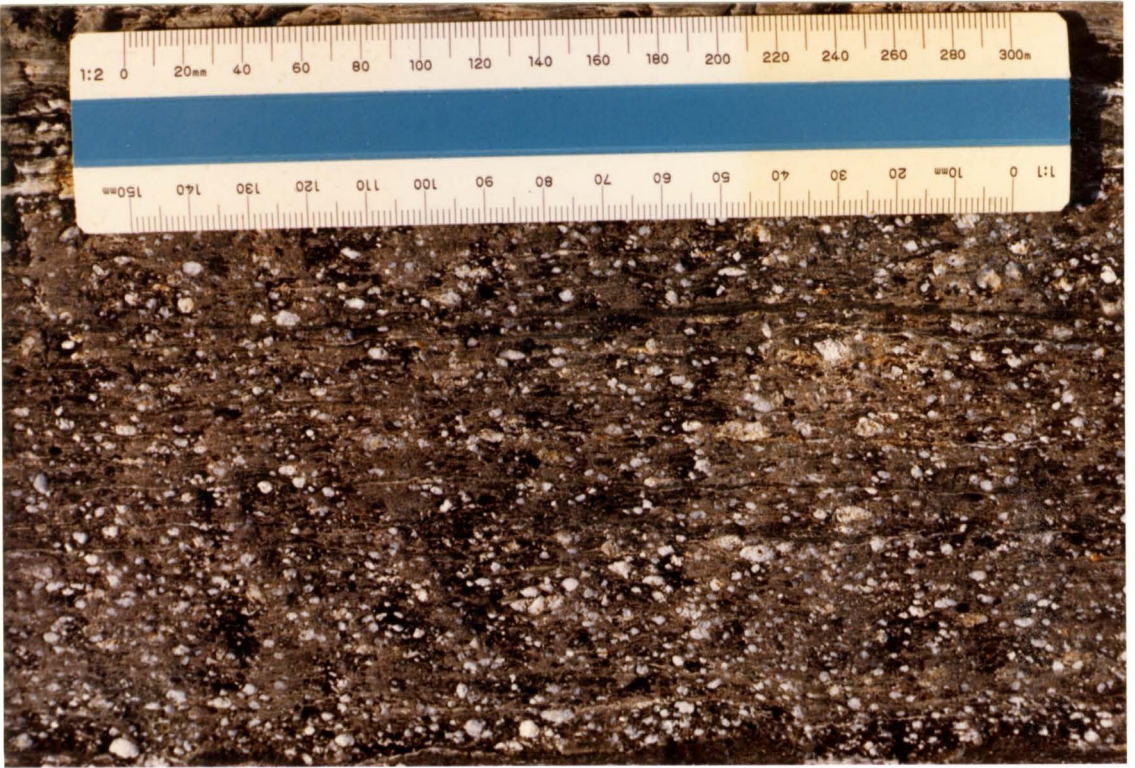
The smallest porphyroclasts are found in zones of darker, finely laminated rock containing very thin layers of both quartz-rich material and amphibolite-rich material (Figure 2). These finely laminated, highly mylonitized zones may be up to 8 cm wide. Zones containing larger porphyroclasts are also present. These are generally wider (up to 30 cm wide) but still show delicate bands of quartz- and amphibole-rich material (Figure 3).

Lenses of amphibolite material are prominent in the more mica-poor rocks of stations SMA-01 and SMA-08 and show two

Figure 2. Finely laminated mylonite layer with fine grained porphyroclasts from SMA-01.

Figure 3. Zone of coarser grained porphyroclasts in protomylonite from SMA-02.







distinct textural behaviors. Briefly, one type displaying "pinch and swell structure" (cf. Ramsay and Hubber, 1983), appears as very stretched lenses tapering gently into narrow, foliation-parallel tails that may continue at widths less than 1 cm for nearly a meter before eventually widening into a new lens. The other type consists of lenses that appear to be made up of many fragments of a highly fractured single parent layer with the fragments now floating in a quartz matrix. Thin (0.2 - 1.0 cm wide) bands of amphibolite-rich material are also seen in these rocks; these conceivably could represent a stretching and concomitant thinning of amphibolite layers that once may have been much thicker continuous dykes. Although no cross cutting relationships can be identified between these amphibolite strips and the host rock, such features may have existed previously only to be obliterated by the high level of strain in these rocks evident from other features.

A more detailed kinematic framework discussion of these and other features follows in chapter 3.

## Thin Section Petrography

Thin sections of the rocks in the study area were studied with the intent of establishing a sequence of formation of internal deformation features through textural observations. A description of the minerals and their textural relationships within the rocks of the study area is presented here. Discussion and interpretation of these features with respect to deformation and metamorphism is left to a later chapter.

**Feldspar porphyroclasts** are the most conspicuous feature in these rocks and range from 0.5 mm to 5.0 mm in diameter. Most porphyroclasts are slightly elongated or oblate in shape and all have thin mantles of tangentially oriented biotite +/- chlorite +/- quartz grains. Muscovite also makes sharp, clean edges with feldspar porphyroclasts whose outlines are too long and continuous to be the result of grain reduction processes. These grains therefore have been thinned at their sides by removal of feldspar material, possibly by chemical processes. In some places porphyroclasts show mantles of highly recrystallized quartz and feldspar surrounding a core of relatively unaltered feldspar. Inclusions of quartz and biotite are very common while rare inclusions of clinozoisite + quartz and carbonate are also present.

Feldspar is also very common in the matrix of the mica-poor rocks in small, augen-shaped grains. These grains

commonly have ragged ends perpendicular to the foliation which are penetrated by fibrous chlorite. These grains have a nearly constant grain diameter throughout the matrix suggesting they may represent the minimum size that could be produced by the grain size reduction processes operating during deformation.

Very narrow, 0.2 to 0.4 mm wide, foliation parallel bands of actinolite are common in the mica-poor rocks. The actinolite grains are diamond-shaped or lath-like with their long axes oriented parallel to the foliation. Grains are boudinaged in places and are bent around irregularities in the foliation in other places. In some instances actinolite grains penetrate the edges of feldspar porphyroclasts.

Biotite is a very common mineral in these rocks and defines the boundaries between quartz ribbons. Grains are present either as long, bent ribbons partially defining the foliation or as very fine, recrystallized flakes that mark zones of locally high shear strain such as quartz ribbon boundaries or "C-surfaces". The biotite flakes frequently penetrate the edges of feldspar porphyroclasts and the tails which protrude outside the porphyroclasts are bent into the surrounding foliated matrix. Biotite is also intimately associated with chlorite in the mica-poor rocks and is present in minor amounts in the mica-rich rocks.

Muscovite is present only in the mica-rich rocks and constitutes approximately 95% of the mica in these rocks.



Biotite is found as thin, cleavage-parallel grains with diffuse boundaries within the muscovite and appears to be consumed by the muscovite. Muscovite is also common as 2-3 mm wide aggregates which are both folded and displaced by C-surfaces.

Dark green chlorite is common in the mica poor rocks. It is always found at the ends of even the smallest feldspar grains, penetrating into the ends of the grains and produce ragged outlines. This suggests a dilatation accompanied feldspar grain-size reduction processes with the chlorite being precipitated in the voids between feldspar fragments. Chlorite is also common in the necks between feldspar pull aparts where it mimics the direction of fragment separation. In the mica-rich rocks, chlorite is common as large, randomly oriented void fillings or in pressure shadows in the quartz veins. The chlorite in these mica-rich rocks is concentrated around veins or can be traced along a fracture or other foliation-parallel conduit back to a quartz vein. Chlorite therefore appears to have been remobilized through fluid flushing during dilatation.

Clinozoisite is most abundant in the more intensely folded rocks of station SMA-02. In this area it is often concentrated into bands. It is intimately associated with quartz and, to a lesser extent, biotite which penetrates the granular grain boundaries. The total absence of feldspar and high concentration of quartz in these bands suggests the

clinozoisite is an alteration product of the feldspars (White et al., 1982). Clinozoisite also occurs more rarely with quartz in inclusions in feldspar porphyroclasts.

Garnets about 0.1 to 0.5 mm in diameter are present in the mica-rich rocks only. Most grains are anhedral and are set in the muscovite rich bands. Most grains are also growth zoned, the zoning being marked by round inclusion trails. The smallest garnets are often euhedral and are totally surrounded by a muscovite matrix.

Rare orthopyroxene grains are found in some thin sections and are surrounded by microcrystalline alteration halos of what appears to chlorite and quartz.

Quartz is common in all sections as ribbons or as veins. It is also common as inclusions in most minerals and forms mantles of recrystallized grains around some feldspar porphyroclasts. Quartz also occurs as worm-like inclusions in myrmekitic feldspars.

Trace minerals include common accessories such as tourmaline in the mica-rich rocks and carbonate as inclusions or fracture fillings in some feldspar porphyroclasts. Opaque minerals are present mostly as anhedral grains except in "protected" areas such as embayments in porphyroclasts where euhedral grains are found.

An odd occurrence of feldspar was observed particularly in one sample of brecciated rock where the well foliated, angular fragments are surrounded by euhedral, zoned, frac-

ture-filling, feldspar. Clinozoisite and radiating worm-like aggregates of chlorite are also common in these veins. In other sections, similar veins cross cut the mylonitic foliation. This occurrence of feldspar, chlorite and clinozoisite suggests these minerals were precipitated by hydrothermal fluids which post date the major period of deformation that produced the mylonitic characteristics of the rocks in the study area.

### Discussion of Petrography

The assemblage of minerals described above indicates the rocks of the immediate study area reached epidote-amphibolite facies conditions during regional metamorphism. The rocks contain minerals indicative of epidote-amphibolite facies conditions (Ehlers and Blatt, 1980; Winkler, 1979) in mafic and pelitic rocks as listed in Table 1 (a greenschist facies overprint is also indicated and is discussed below). This is in agreement with regional metamorphic trends that confine the rocks of the study area to amphibolite grade conditions (Henderson et al., 1987). The mafic component is probably due to the presence of the amphibolite rocks which are present throughout the straight zone. The high calcium minerals such as tremolite-actinolite and clinozoisite probably represent a high calcium content of the same amphibolitic rocks possibly



**Table 1:** Table of minerals typical of Epidote-amphibolite and Greenschist facies conditions in the study area

| <u>Epidote-amphibolite Facies</u> | <u>Greenschist Facies</u> |
|-----------------------------------|---------------------------|
| <b>Mafic Minerals</b>             |                           |
| epidote (clinozoisite)            | chlorite                  |
| almandine garnet                  | actinolite                |
| quartz                            | clinozoisite              |
| tremolite-actinolite              | quartz                    |
| (Ca-rich mafic rocks ?)           |                           |
| <b>Pelitic Minerals</b>           |                           |
| almandine garnet                  |                           |
| chlorite                          |                           |
| muscovite                         |                           |
| biotite                           |                           |
| quartz                            |                           |

from calcium rich plagioclase and/or pyroxene.

Feldspar textures described in chapter 3 indicate that deformation continued through relaxing metamorphic conditions. Epidote minerals (ie. clinozoisite) are produced during retrograde adjustments associated with dynamic metamorphism according to Deer, Howie and Zussman (1982). These same authors state that the formation of epidote is favoured by shearing stresses. The epidote is involved in the deformation at all levels and is especially common in an area of tightly folded rocks. The clinozoisite is therefore a product of reactions that took place during deformation, probably as conditions fell below epidote-amphibolite facies conditions. Chlorite also formed coevally with deformation as indicated by its fibrous form in the necks between extensional pull aparts. Winkler (1979) states that the assemblage  
chlorite + clinozoisite +/- actinolite +/- quartz  
is typical of greenschist facies conditions. He also states that chlorite is easily formed as a secondary alteration product (of biotite or hornblende), especially in rocks subjected to post-metamorphic deformation or fracturing. The presence of this assemblage therefore is attributed to reactions that took place as metamorphic conditions fell to greenschist facies.

Other textures indicating coeval mineral formation and deformation were also noted. These include syn-deformation crystallization of biotite, muscovite and quartz. Further

refinements of internal timing are presented in a discussion of kinematic indicators in chapter 4.



## Chapter 3: Kinematics

### Introduction

In recent years much interest has been shown in, and much time devoted to, the problem of determining the sense of movement in ductile and brittle-ductile shear zones. The problem has been approached from different angles but always with the intent of interpreting mesoscopic and microscopic fabrics in terms of a bulk flow or shear direction. The interpretations often attempt to determine possible domains or positions of principal strains and suggest mechanisms which may have produced the structural fabrics or elements. Such kinematic and dynamic analyses of naturally deformed rocks have been undertaken in terms of progressive deformation (eg. Berthe et al., 1979; Berthe and Brun, 1980; Simpson, 1983), theoretical controls (eg. Lister and Williams, 1980), specific classes of deformation features (Hanmer, 1986; Lister and Snoke, 1984; Passchier and Simpson, 1986) and as general summaries of the structures and their implications (Platt and Vissers, 1980; Simpson and Schmid, 1983; Simpson, 1986; Stauffer, 1970). A similar structural analysis of this study area has been attempted with emphasis on the kinematic and dynamic implications of

the structural fabrics aided by comparisons with the findings of similar previous studies.

There are two steps in such a kinematic analysis. The first is to describe the structural elements with respect to their nature, orientation and geometric relationships. The second is to interpret the data based on the existing theoretical and empirical observations with the intent of determining principal strain domains and possible mechanisms responsible for the development of the observed fabric (O'Donnell, 1986).

Analysis of the study area with these objectives in mind will be discussed in two parts. The first will deal with features observable at the scale of the outcrop, the mesoscopic structure. The second will deal with features observable in thin section, the microscopic structure. Structural analysis at this scale has not been previously attempted in the study area so the general structural fabric of the Artillery Lake area will be compared with that noted by others at larger scales (Henderson et al., 1987; James, 1986).

The study area is located within the "straight zone" which is a zone of porphyroclastic migmatitic metasediments and amphibolitic rocks that are characterized by a north-northeasterly trending foliation with steep dips to the southeast and a steep, northeasterly plunging lineation. In the study area, the straight zone deviates from its trend of  $020^{\circ}$  typical of the rest of the domain, swinging to approximately



060°. This may cause complications in interpretations of the strain features with respect to the rest of the Artillery Lake map area but a simplified view of this kink in the straight zone as simple rotation of the fabric elements about a sub-perpendicular axis will be adopted.

The rocks of the study area are more highly strained than elsewhere in the "straight zone". Rocks typical of the "straight zone" are dominantly porphyroclastic and do not display the mylonitic characteristics seen in the rocks of the study area. This contrast in deformed state may be due to the kink in the "straight zone" mentioned above but no evidence for this was noted during regional mapping. Kinematic indicators viewed in the plane of the outcrop imply a dextral component of motion along a horizontal axis while evidence for a significant sub-vertical component of motion is noted from thin section observation.

### Mesosopic Structures

This section describes the structures observed in outcrop including a set of 4 kinematic indicators. These indicators are extensional shear bands, asymmetric porphyroclast tails, asymmetric folds and boudinaged amphibolite lenses. The most reliable indicators of bulk shear sense are the extensional shear bands and the asymmetric folds; both of



these structures indicate a dextral sense of shear in the plane of the outcrop with remarkable consistency. The asymmetric porphyroclast tails and boudinage by themselves are less reliable.

Two primary strain features present in outcrop are the foliation and the lineations. The foliation is a well developed proto-mylonitic to mylonitic foliation defined by discrete, sometimes delicate, layers of stretched quartz and darker amphibolitic material. In some places these layers are interrupted by or wrap around feldspar porphyroclasts and may taper to fine terminations. The foliation is rectiplanar forming parallel, nearly rectangular blocks of heaved or fractured rock that appear to have parted along foliation planes defined by high mica concentrations. The foliation is very consistent at the scale of this study area, not varying more than  $10^\circ$  either side the mean trend of  $056^\circ$  (Figures 4 & 5, Table 2).

Closer examination of the foliation reveals gentle undulations which have an open fold shape and wavelengths of approximately 2.0 mm to 2.0 cm. These may be a smaller scale expression of the folding observed in the mica-rich rocks of station SMA-02. Dips in the unit are generally very steep to the southeast with local variations dipping to the northwest. Foliation surfaces are bumpy or knobby due to the protrusions of the more competent feldspar porphyroclasts but no rodding

Figure 4. Map of study area with structural data and station locations. Inset showing location of study area within the Artillery Lake area.

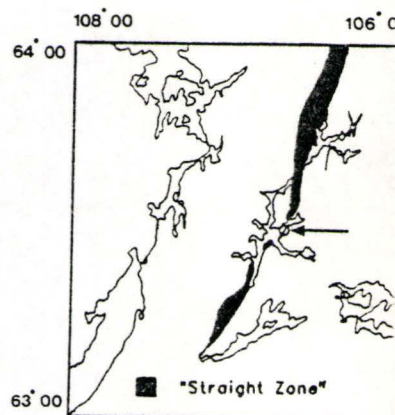
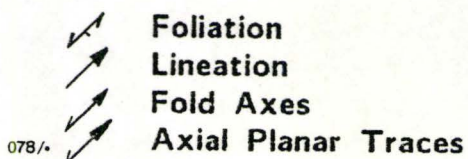
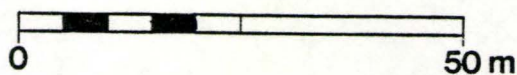
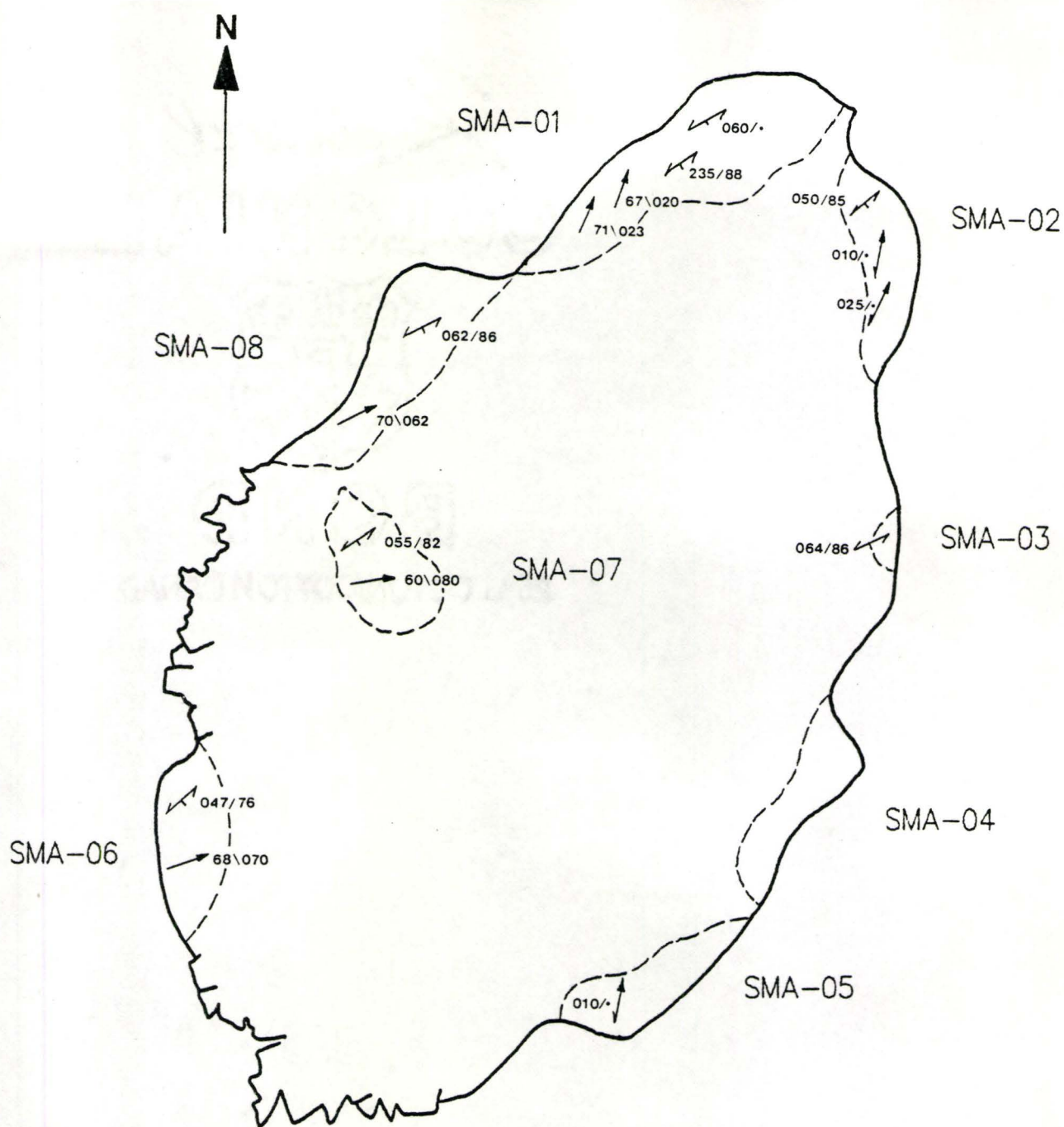




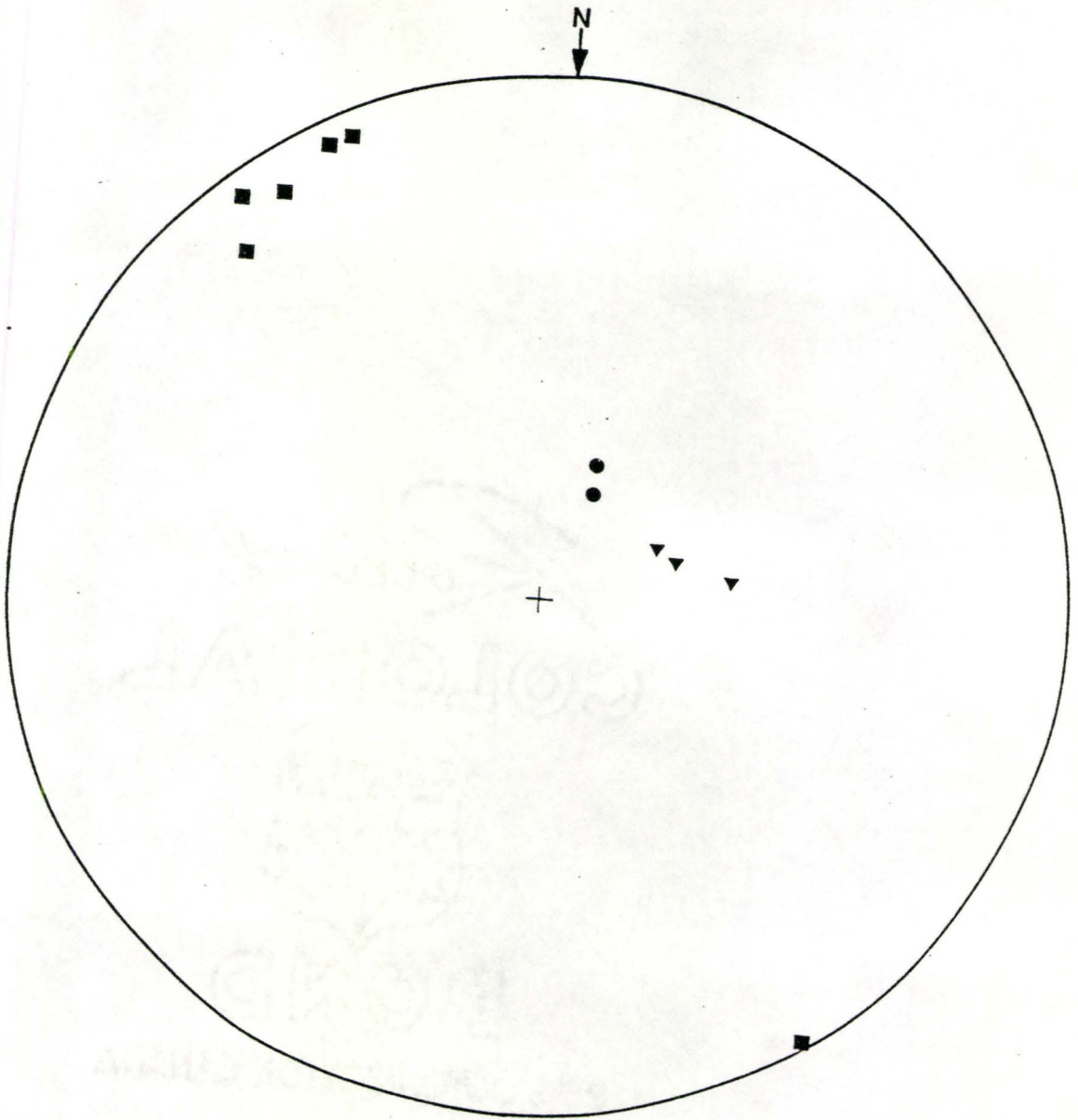
Table 2: Table of Structural Data

| <u>Station</u> | <u>Foliation</u> | <u>Fold Axes</u>        | <u>Lineation</u> |
|----------------|------------------|-------------------------|------------------|
| SMA-01         | 235/88           | 71\023                  | -                |
|                | 060/___          | 67\020                  | -                |
| SMA-02         | 050/85           | (010/___ -<br>025/___)* | -                |
| SMA-03         | 064/86           | -                       | -                |
| SMA-05         | -                | 010/___*                | -                |
| SMA-06         | 047/76           | -                       | 68\070           |
| SMA-07         | 055/82           | -                       | 60\080           |
| SMA-08         | 062/86           | -                       | 70\062           |

---

"\*" Denotes trace of Axial Plane  
in plane of outcrop

Figure 5. Stereoplot of structural data in study area.



- Poles to Foliation
- Fold Axes
- ▼ Lineations

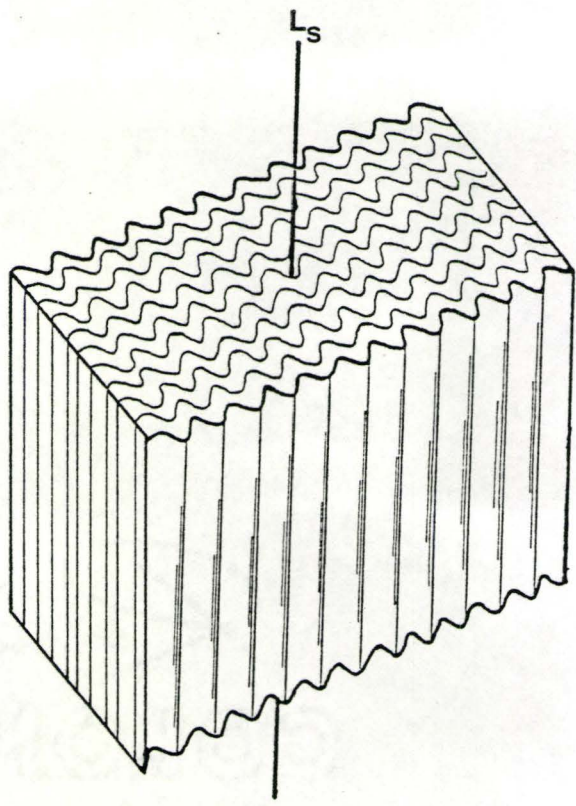


of feldspars or other minerals is visible in these particular surfaces.

A lineation plunging  $65^{\circ}$  to  $70^{\circ}$  at azimuths of  $062^{\circ}$  to  $080^{\circ}$  is common in many foliation surfaces but is by no means ubiquitous. Another more poorly defined lineation oriented sub-horizontally, plunges approximately  $5^{\circ}$  to the northeast in the plane of the outcrop but this lineation is poorly expressed in these rocks and cannot be accurately defined. The steeply plunging lineation ( $L_3$ ) is expressed in two different ways. In some instances it appears as a stretching lineation on the surface of some quartz veins or quartz-rich foliation-parallel surfaces. In other surfaces it is formed by the long synclinal troughs and anticlinal ridges of small open folds present in some of the rocks in the study area. This corrugation lineation (Figure 6) extends for a maximum of 5.0-6.0 cm down foliation surfaces. This is similar to a corrugation lineation described by Vauchez (et al., 1987).

Large (0.5 m) to small (1.0 cm) extensional shear bands or "C-surfaces" cut the foliation at angles of roughly  $40^{\circ}$  are a common extensional feature in the study area. These extensional shears are best recognized by discontinuities in amphibolitic layers and the shears are imagined as discordant zones of locally high shear strain which curve back into concordance with the foliation at their terminations (Figure 7). The extensional shears are commonly visible at the outcrop scale only in the mica-poor rocks and are especially

Figure 6. Block diagram illustrating nature of corrugation lineation.





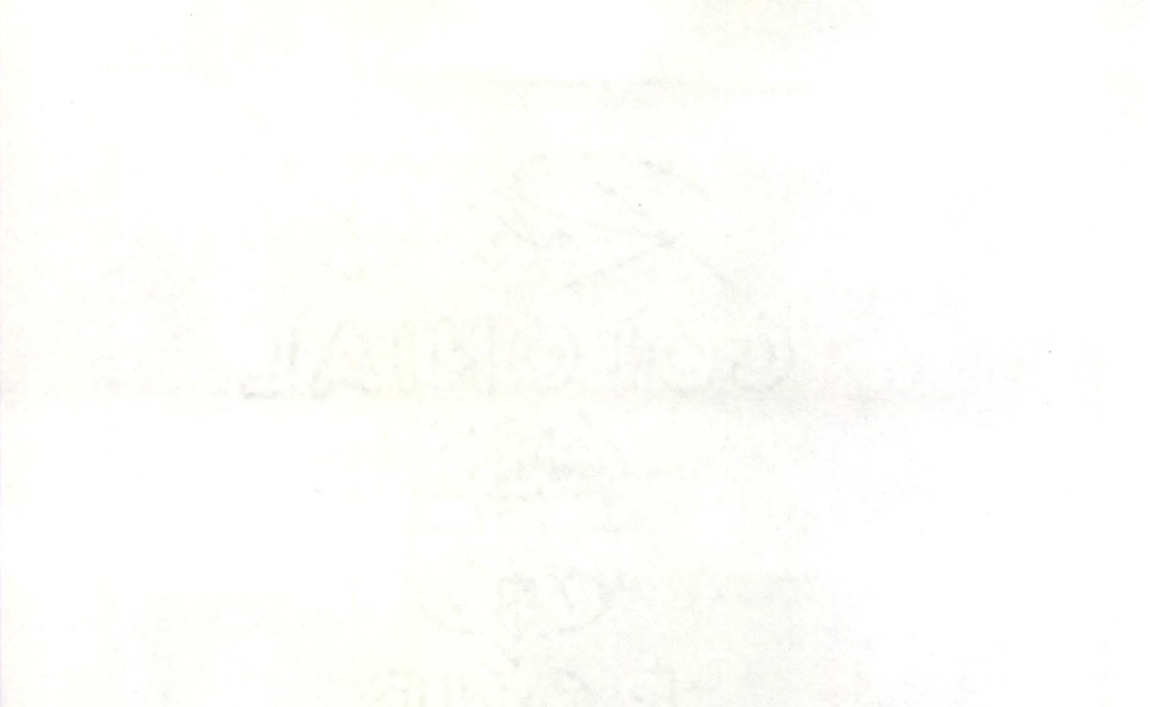
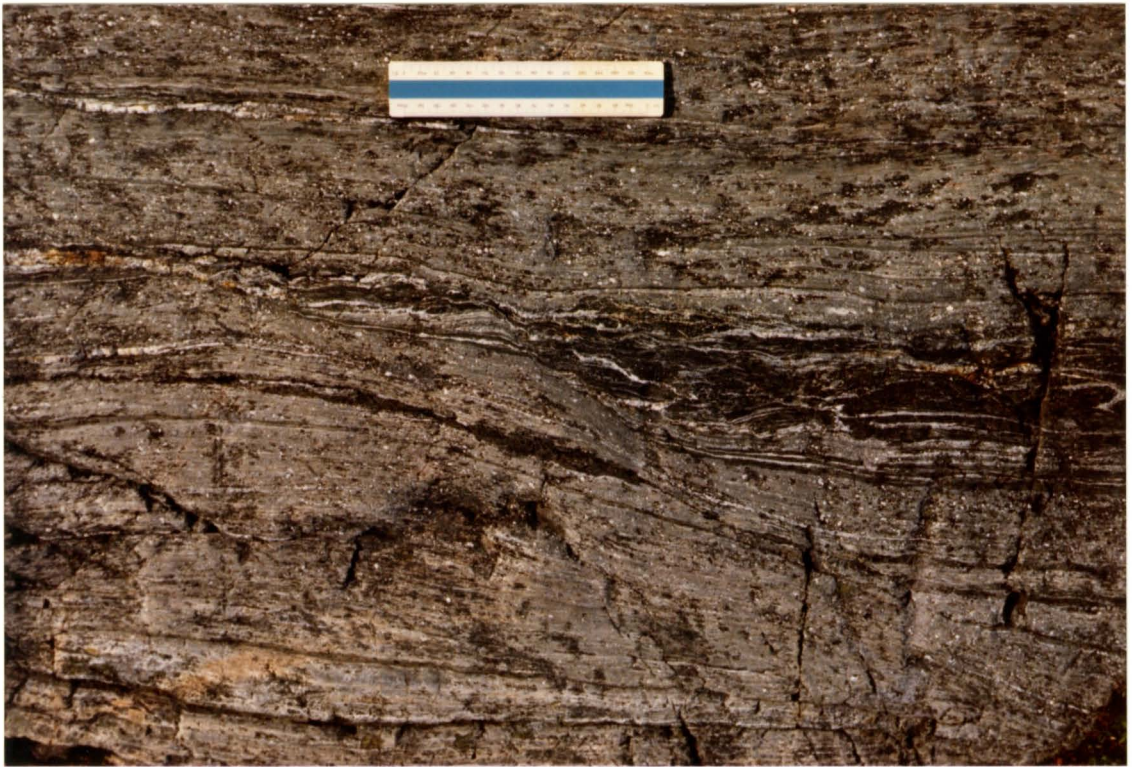


Figure 7. Ductile shear or "C-surface" cutting foliation from upper left to lower right. Scale is 15 cm long. Station SMA-01.



common around heterogeneities in the rock such as amphibolite lenses or quartz veins. These ductile shear bands do not form a penetrative fabric; rather, they are singular, irregularly spaced features and where visible in a vertical plane are continuous only over a few centimeters. All these extensional shears indicate a dextral sense of displacement. The shear or C-surfaces (Berthe et al., 1979) and the mylonitic foliation intersect at a point forming an "arrowhead" which points in the general direction of bulk flow. An alternate view considers deflections of the foliation. In this situation the shears step down to the right indicating right lateral slip along the C-surfaces.

The shear bands are intimately associated with another kinematic indicator. These are asymmetrical pull aparts in the amphibolite layers and are similar to structures described by Hanmer (1984) as Type 1 and Type 2 asymmetrical pull aparts. The more symmetrical pinch and swell structure (cf. Ramsay, 1983) or Hanmer's Type 2 asymmetrical pull aparts are formed of lenticular lenses of amphibolite material which gently taper to peaked terminations or may be connected to another lens of material by long, thin, foliation-parallel strips of the same parent material. This style of boudinage occurs dominantly within the very straight, quartz/feldspar mylonitic rocks (Figure 8a). The other style of boudinage (Hanmer's Type 1 asymmetrical pull apart) is a slightly more brittle expression of extension where the



original parent amphibolite lens is highly fragmented, the fragments being surrounded by a quartz matrix. In the necks between some of these boudins, antithetic shear displacements between some of the more angular fragments can be discerned (Figure 8b). The boudins in these areas tend to be slightly rotated into the direction of shear (dextral) whereas in the type-2 asymmetrical pull aparts, the separated fragments are back rotated in a direction opposing passive shear rotations. The asymmetrical pull aparts by themselves are not definitive kinematic indicators in the study area. However, when other indicators are considered together with the Type 1 and Type 2 pull aparts, the pull aparts provide supporting indications of dextral shear.

In the more mica-rich rocks feldspar porphyroclasts are generally larger and they have their long axes oriented at angles of approximately  $025^{\circ}$  to the dominant foliation. Many have tails which trail off into the foliation (Figure 9a) but these features may be related to the folding that dominates the rocks in this outcrop (SMA-02). The porphyroclasts are aligned along the north trending limbs of the small open folds while the tails are drawn out into the nose and the west trending limbs of the folds (Figure 9b). In some places, the porphyroclasts appear closely related to thin folded layers of the migmatite leucosome (quartz/feldspar-rich) material where in the more tightly folded cores, the layers undergo stretching and consequent thinning leading to

Figure 8a. Symmetrical "pinch and swell" pull apart in amphibolite layer in straight mylonite. Scale is 15 cm. Station SMA-01.

Figure 8b. Brittle asymmetrical pull apart in quartz veined amphibolite layer. Station SMA-01. 7



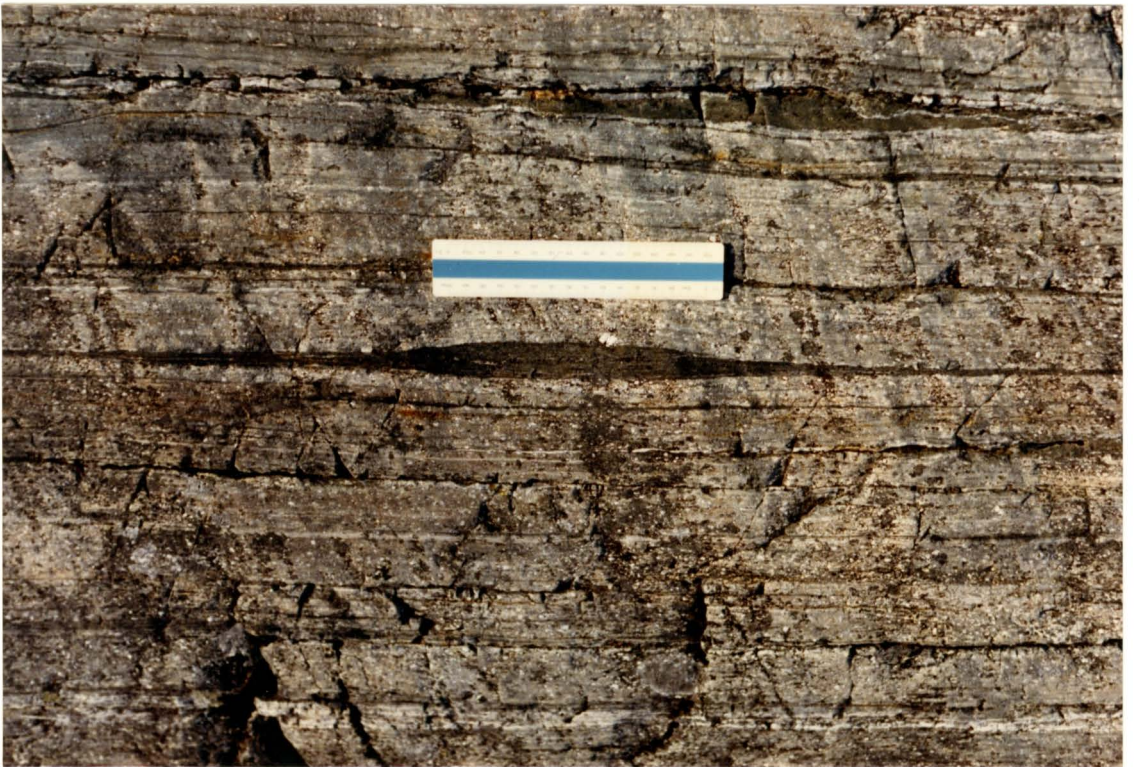




Figure 9a. Asymmetrical tails on feldspar porphyroclasts in mica-rich rocks. Arrow points North. Station SMA-02.

Figure 9b. Porphyroclast formed from stretched quartz-feldspar layer aligned along the north trending limb of small fold. Scale is 15 cm. Arrow points North. Station SMA-02.

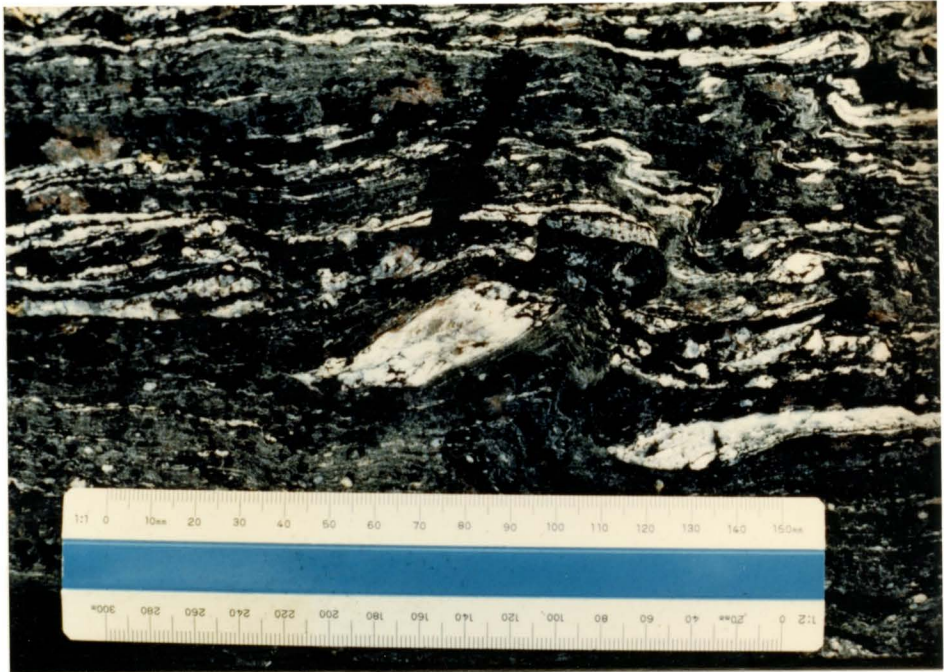
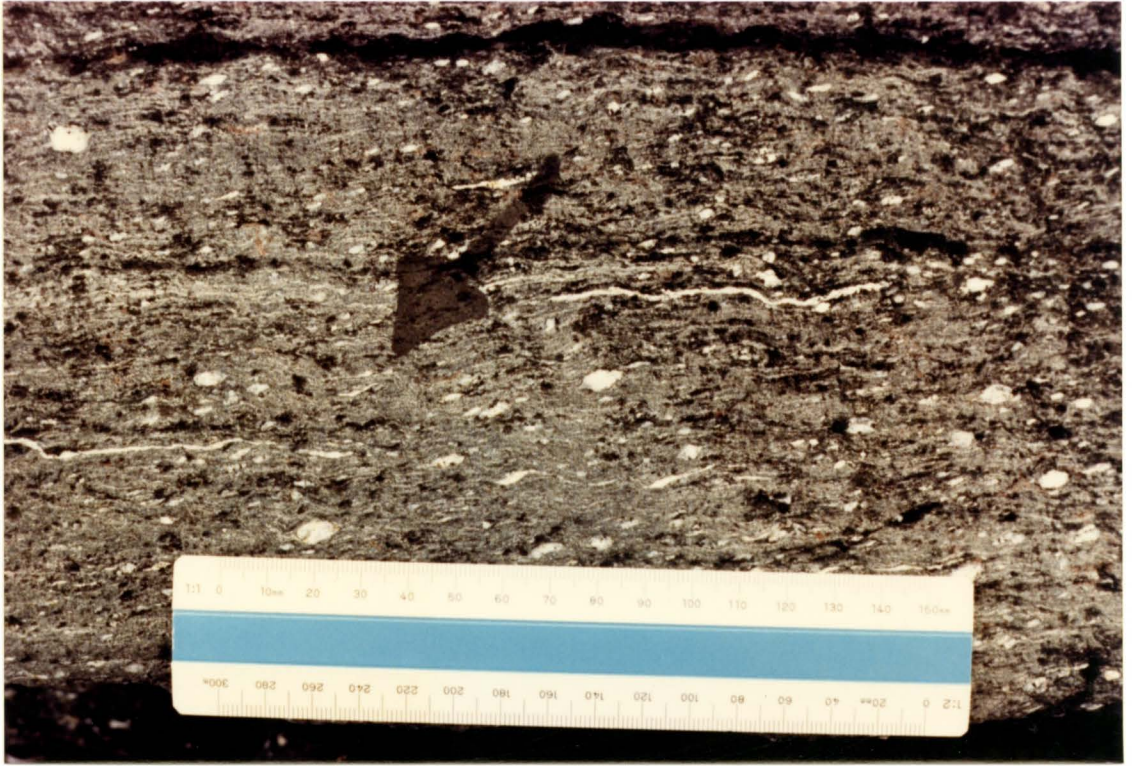
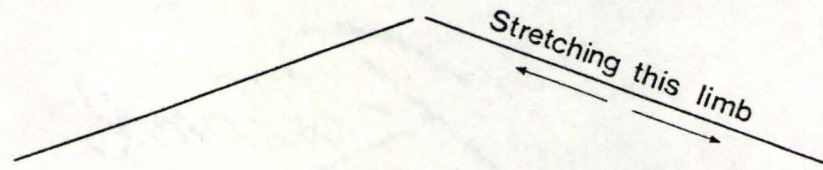
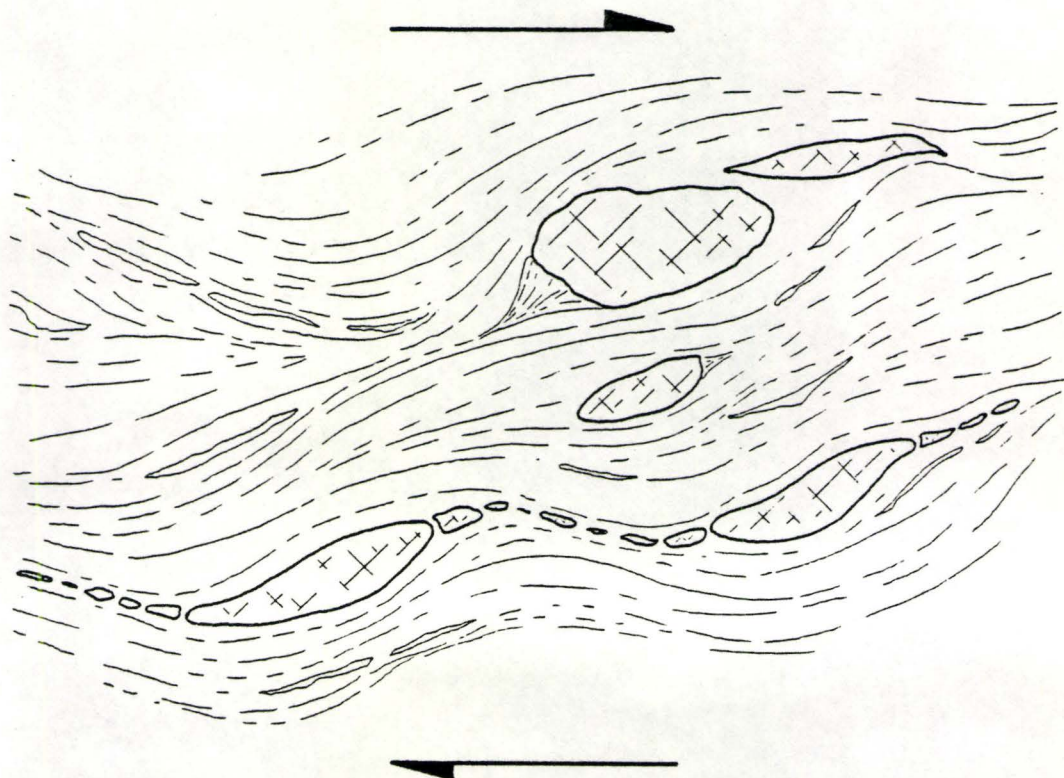




Figure 10. Diagram showing stretched quartz-feldspar layers along one limb of folds due to right lateral shear (cf. Figures 9a and 9b).





isolated, elongate, sigmoidal fragments of quartz/feldspar-rich material (Figure 10).

The asymmetrical folds in the study area have their fold axes oriented near 020/70 and axial planar traces viewed in the plane of the outcrop varying from 010° to 025°. The folds are marked by folded quartz/feldspar-rich layers. In some places they are very open (Figure 11a) while in others they are very tight, approaching an isoclinal shape (Figure 11b). In places where these folds are expressed only in the mica-rich layers they tend to be very open and may, as was previously suggested, be responsible for the preferred orientation of some porphyroclasts. These smaller folds have amplitudes of approximately 0.5 cm and wavelengths of approximately 2.0 cm whereas others may have 4.0 to 6.0 cm amplitudes and 10.0 to 15.0 cm wavelengths. In other areas (parts of SMA-02 and SMA-03) the folds are very contorted and folds pile on top of one another, tending to look ptygmatic in character. The vergence of these folds still indicates a dextral sense of shear displacement. The larger folds appear to be most common in the more mica-rich rocks of the area while the more competent quartz/feldspar-rich rocks exhibit only smaller folds as a "crinkling" of the foliation. The vergence of nearly all these folds in the area is consistently to the southwest indicating a dextral sense of bulk flow in the plane of the outcrop.



Figure 11a. Open asymmetrical folds with southwest vergence. Station SMA-02.

Figure 11b. Tighter asymmetrical folds with southwest vergence. Station SMA-02.





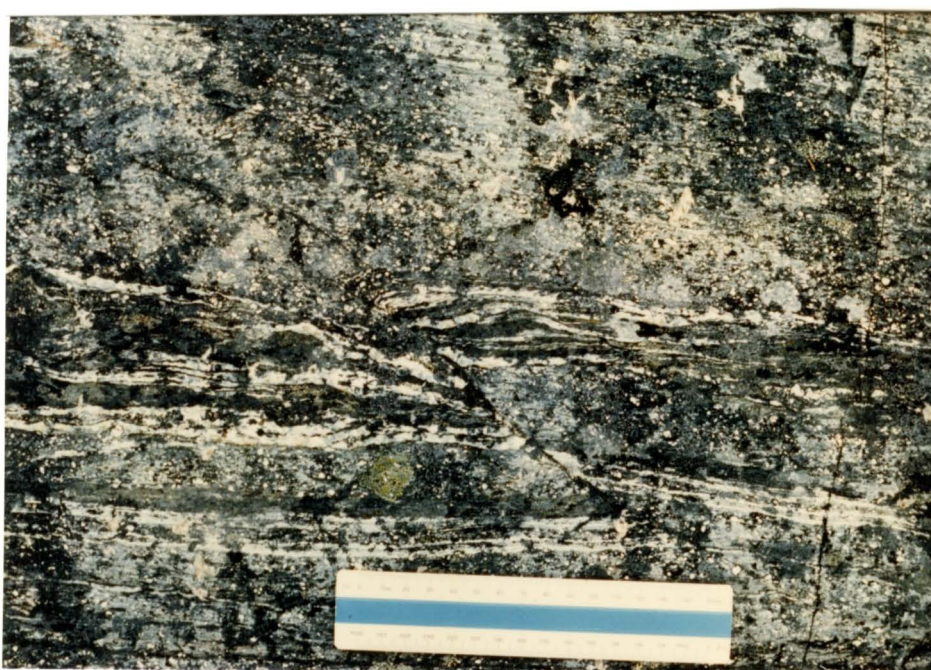
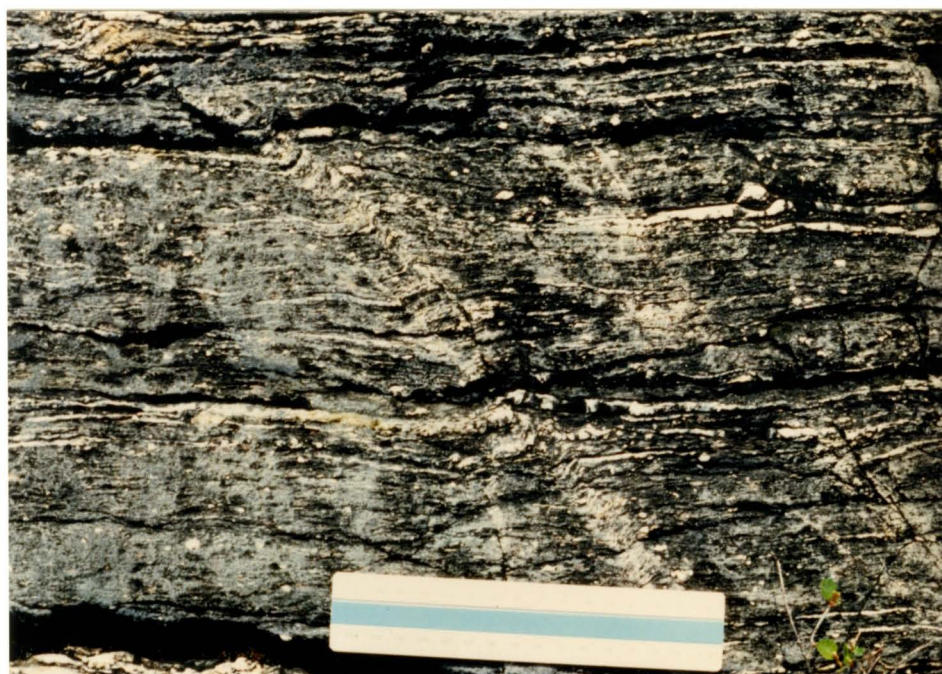
Indicators of a vertical component of flow in these rocks were generally not visible in outcrop. However, in one particular location (SMA-07) a vertical surface was examined looking to the northeast ( $060^{\circ}$ ). Shear bands viewed in this surface indicate a shear displacement with the southeast block being downthrown. This is inconsistent with the regional view of vertical components of motion which suggest that the more eastern domains are deeper exposures which have been upthrown. If the "straight zone" is an expression of the Thelon Front then this inconsistency may be a local variation only. Further discussion of the vertical component of shear displacement is left to later chapters where this dilemma is partially resolved.

Brittle and brittle-ductile deformation features including fractures and kink bands showing sinistral displacement were also observed in outcrop. The kink bands were observed at stations SMA-02 and SMA-05 and had trends  $085^{\circ}$  and  $090^{\circ}$  (Figure 12a). The motion accommodated by these kink bands is in a sinistral sense and the smaller foliation crenulations are deformed within the kink bands. Brittle-ductile faults with trends varying little either side of  $090^{\circ}$  have cut and sinistrally displaced some folds within the foliation (Figure 12b). These folds presumably were initiated as ductile features and at some later point moved into a brittle fracture regime. Alternatively the deflections of the foliation into the fault plane in an anti-clockwise sense in

Figure 12a. Kink band trending  $085^{\circ}$  indicating left lateral (sinistral) compressive shear. Station SMA-02.

Figure 12b. Brittle-ductile, sinistral sense fault offsetting amphibolite layer. Fault trend is  $100^{\circ}$ . Station SMA-01.







areas immediately adjacent to the fault plane could be the result of locally ductile behaviour creating drag folds. Both the kink bands and the faults have trends near  $090^{\circ}$  and sinistral displacements. It is therefore likely that both represent a late event in the study area, probably related to Bathurst Fault tectonics.

### Microscopic Structures

This section describes the structures observable in thin sections. Most features were observed in thin sections cut subparallel to the lineation and perpendicular to the foliation unless otherwise stated. Kinematic indicators include extensional features that generally give reliable indications of bulk flow or shear displacement. The assemblage includes extensional shear bands or C-surfaces (Berthe et al., 1979), microfaulted feldspar porphyroclasts, feldspar pull aparts, mica "fish" (Lister and Snoke, 1984), asymmetrical porphyroclast tails, and asymmetrical microfolds. Other strain features such as deformation twins in feldspar porphyroclasts, quartz ribbons, and subgrain fabrics are also described. Interpretation of these features is left for discussion in a following section.

**C-surfaces** (Berthe et al., 1979) or extensional crenulation cleavages (Platt and Vissers, 1980) are common features

in thin sections both perpendicular and parallel to the stretching lineation ( $L_S$ ). These occur as single microfaults or small-scale ductile shear zones that form dominantly in one set at low angles to the mylonitic foliation. In some samples these surfaces form subparallel sets but usually occur as single discrete zones of intense ductile shearing. These are marked most commonly by fine grained muscovite but may also be marked by biotite and/or chlorite. These surfaces often "offset" markers in the foliation such as amphiboles or micas and most of these surfaces or cleavages occur at angles of  $20^\circ$  to  $40^\circ$  to the mylonitic foliation (Figure 13a). The surfaces themselves tend to be rather discontinuous and may anastomose in and out of the mylonitic foliation. At their terminations the surfaces tend to asymptotically curve into and merge with the mylonitic foliation (Figure 13b). The surfaces rarely extend over more than the width of two or three grain aggregates whose boundaries are defined by foliation parallel, recrystallized mica flakes.

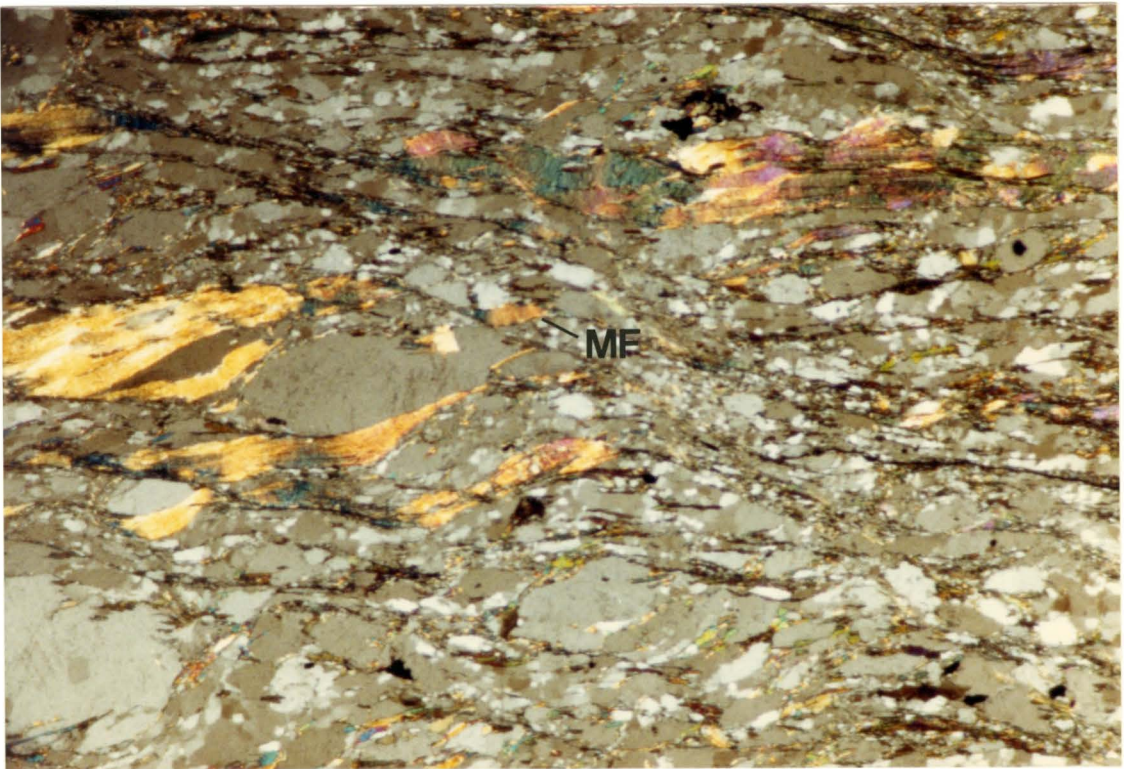
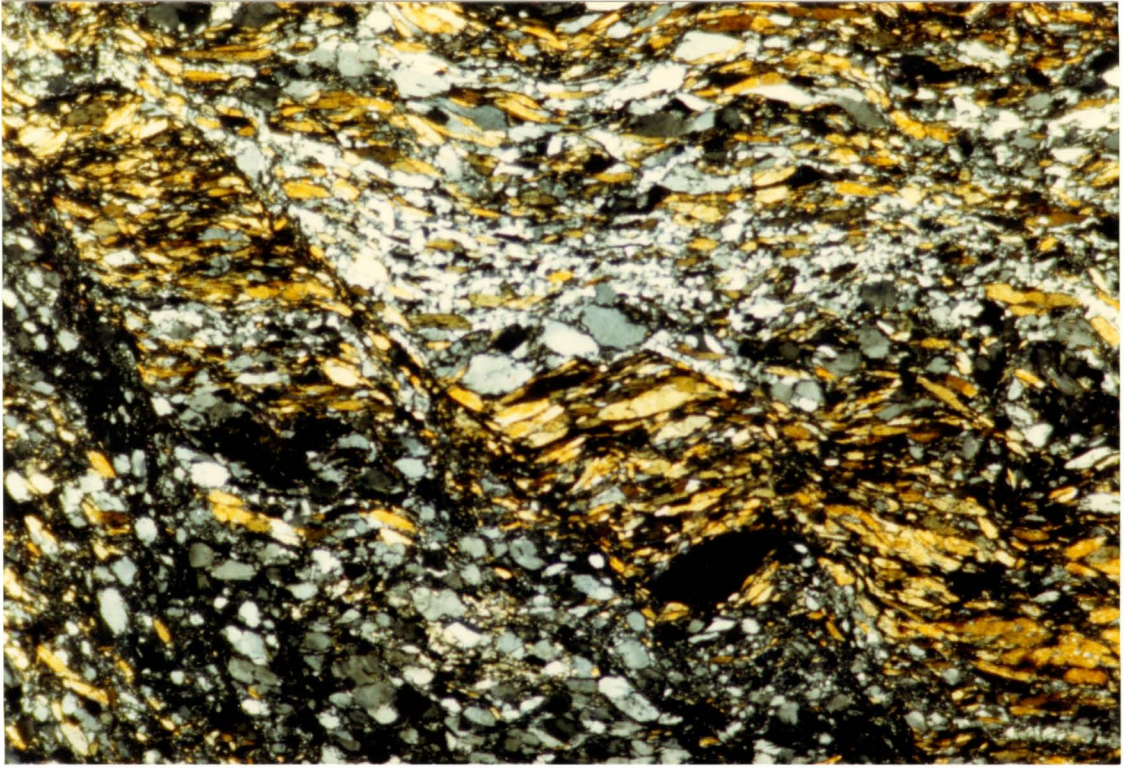
In some thin sections of the more mica-rich rocks (eg. SMA-02-D) a "C&S fabric" similar to the one described by Lister and Snoke (1984) has developed. Here the dominant foliation is defined by elongate feldspars, quartz ribbons and mica flakes and this foliation is cut by surfaces of microscopic discontinuities. These C-surfaces are often defined by the tails of mica "fish" (Lister and Snoke, 1984) that form between these zones of locally very high shear



Figure 13a. C-surface cutting and displacing amphibolite layer. Back rotation of the central "block" of amphibolite in an anticlockwise sense is evident. Field of view is 2.5 mm by 4.0 mm, 240x magnification, t/s SMA-01-E.

Figure 13b. C and S Fabric. C-surfaces cut across photo from upper left to lower right. S-surfaces are horizontal. Back rotation of blocks between C-surfaces evident at left centre. Mica "fish" (MF) visible between two C-surface. Field of view 2.5 mm by 4.0 mm, 240x magnification, partially crossed polars, t/s SMA-02-D.







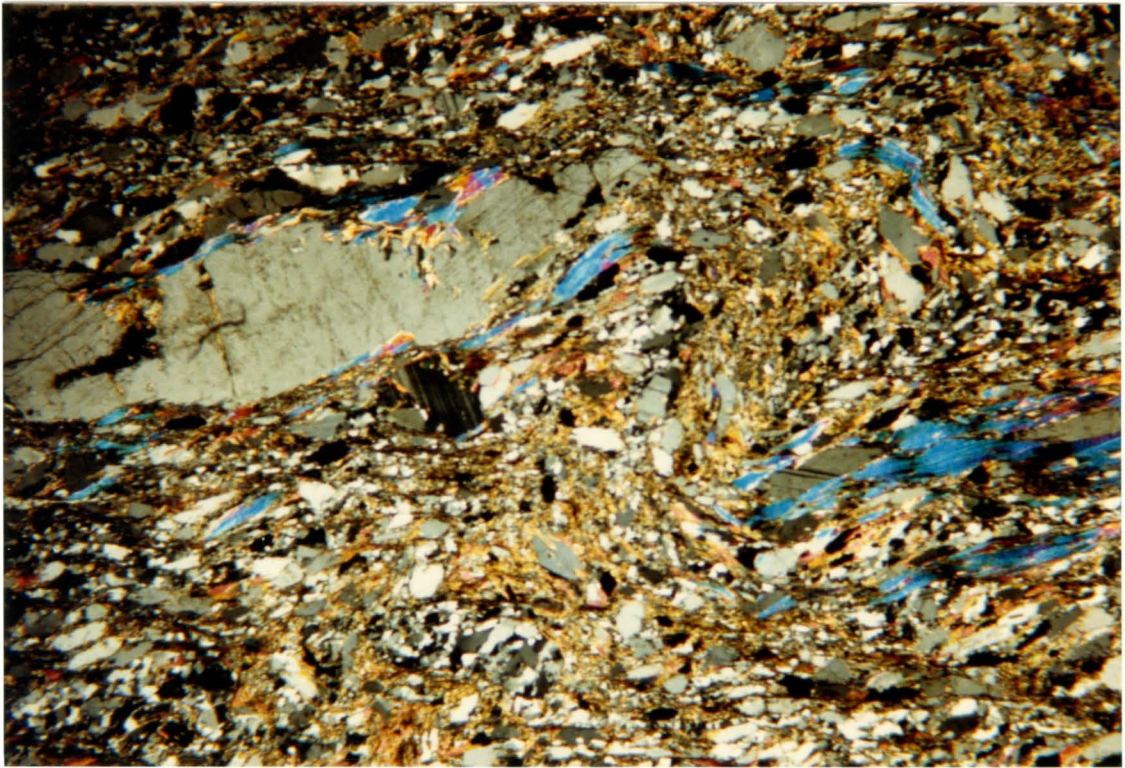
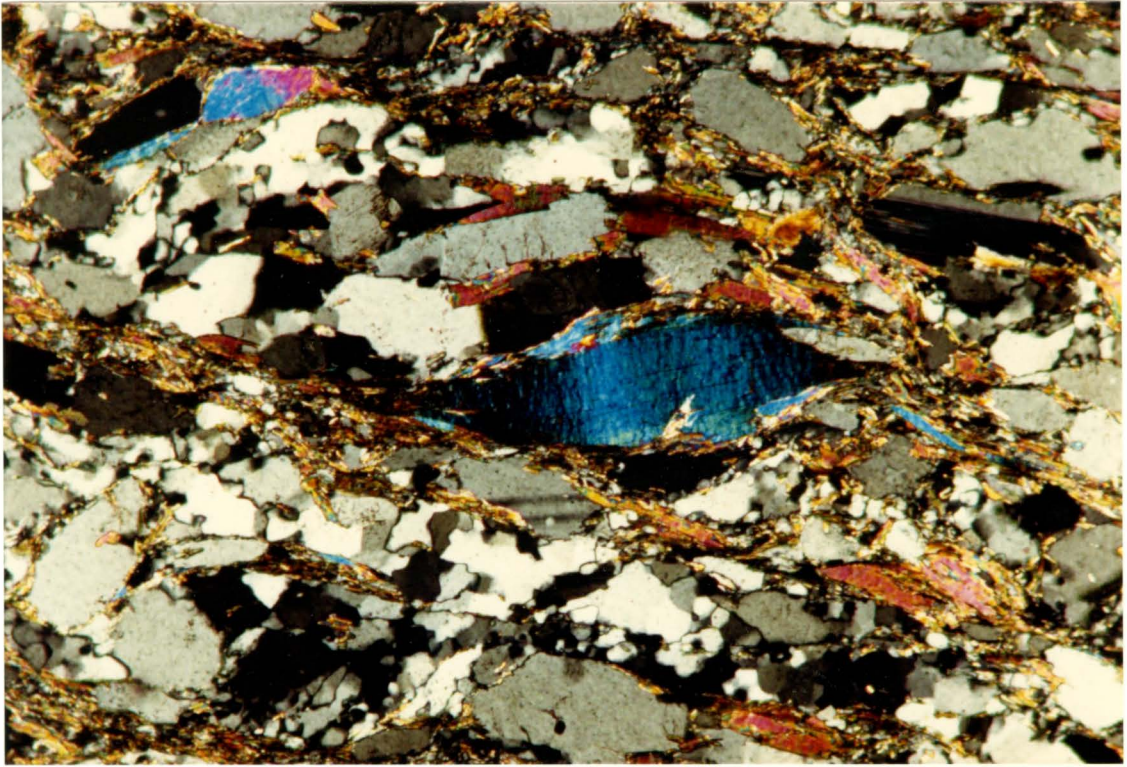
strain. Poorly defined subparallel arrays are formed by these surfaces at shallow angles ( $30^{\circ}$ - $40^{\circ}$ ) to the foliation and only rarely do these surfaces appear to be penetrative, cutting across several grain aggregate boundaries (Figure 13b). These two features may essentially be treated as identical except that the C&S fabric is characterized by the presence of the mica "fish". Mica "fish" are defined by Lister and Snoke (1984) as pre-kinematic mica grains (biotite or muscovite) aligned parallel to the foliation which are sheared or boudinaged by crystal-plastic processes to form asymmetrically shaped fragments (Figure 14). Similar "fish" are observed in study area. As a result of the right-lateral slips along shear surfaces, the "fish" are tilted back against the sense of shear. The "fish" thus indicate a dextral sense of shear indicated by the step-down to the right along the shear slip surfaces.

Microfolds were observed in thin sections oriented perpendicular to the stretching lineation ( $L_S$ ). In the mica-rich rocks, the mica grains are broken at the apices of the tighter folds (Figure 15). The shorter, sometimes overturned limbs are defined by finer grained muscovite grains. In the mica-poor rocks, the folds are defined by bent, unbroken quartz ribbons and thin seams of biotite and chlorite. Similar to the meso-folds observed in outcrop, these micro-folds show a consistent vergence that intuitively indicates dextral shear.



Figure 14. Mica "fish" between two C-surfaces. Mylonitic foliation nearly horizontal. Field of view 1.0 mm by 1.5 mm, 630x magnification, t/s SMA-02-D.

Figure 15. Asymmetrical microfold showing showing extension of material in tight fold cores. Field of view 4.0 mm by 6.0 mm, 148x magnification, t/s SMA-02-D.





The textures described above indicate mechanisms of a ductile character but other brittle mechanisms also operated to produce textures which provide kinematic information. The ductile processes operate in soft or incompetent mineral species such as micas or quartz whereas the brittle processes are confined to the more competent feldspar porphyroclasts.

"Pull apart" structures were observed dominantly in thin sections oriented subparallel to the stretching lineation (Table 3). Most appear to be the result of brittle processes, though some exhibit a combination of brittle and ductile characteristics. This texture is preferentially displayed in the larger porphyroclasts. They appear to have moved within the matrix material by slip along the mica/chlorite mantles which surround the porphyroclasts. Some of these pull apart porphyroclasts show a slightly ductile character indicated by the thinned waists in the parts of the fragmented porphyroclasts that are immediately adjacent to the fractures. The fractures in these pull aparts are subperpendicular to the stretching direction and probably formed as tensile fractures. The gap between fragments typically is filled with recrystallized material most commonly composed of a dark green chlorite (+/- feldspar +/- quartz +/- biotite) whose fibrous nature suggests the lines of motion of the separated fragments (Figure 16a). The fibers of chlorite often penetrate the irregular to serrated fracture walls of the porphyroclasts and are subperpendicular to the fracture



**Table 3.** Table of thin section orientation with respect to stretching lineation ( $L_S$ ) vs dominant microstructure

| <u>Thin Section</u>   | <u>Orientation</u>                    | <u>Structure</u>           |
|-----------------------|---------------------------------------|----------------------------|
| SMA-01-E              | perp. to $L_S$                        | C-surfaces                 |
| SMA-01-H              | perp. to $L_S$                        | faulted<br>"porphs"        |
| SMA-01-M              | parallel to $L_S$                     | pull aparts                |
| SMA-01-N              | parallel to $L_S$                     | pull aparts                |
| SMA-01-O <sub>a</sub> | parallel to $L_S$                     | microfolds                 |
| SMA-01-O <sub>b</sub> | perp. to $L_S$                        | microfolds                 |
| SMA-01-S <sub>a</sub> | perp. to $L_S$                        | faulted<br>"porphs"        |
| SMA-01-S <sub>b</sub> | parallel to $L_S$                     | pull aparts                |
| SMA-01-T <sub>a</sub> | perp. to $L_S$                        | faulted<br>"porphs"        |
| SMA-01-T <sub>b</sub> | parallel to $L_S$                     | pull aparts                |
| SMA-01-U <sub>a</sub> | perp. to $L_S$                        | faulted<br>"porphs"        |
| SMA-01-U <sub>b</sub> | parallel to $L_S$                     | pull aparts                |
| SMA-02-D              | perp. to $L_S$                        | C-surfaces +<br>microfolds |
| SMA-02-F <sub>a</sub> | perp. to $L_S$                        | C-surfaces +<br>microfolds |
| SMA-02-F <sub>b</sub> | approx. 30°<br>to $L_S$<br>(vertical) | C-surfaces                 |

(all thin sections cut perpendicular to foliation)

walls. During deformation some fractured fragments may be displaced due to subsequent interference with adjacent grains and such fragments are joined by oblique fibers of chlorite that mimic the local displacement direction (Figure 16b). Recrystallized quartz and feldspar are both present in these neck areas and normally are confined to the edges or sharp corners on the fragmented grains. The fibrous chlorites in the neck areas often form a spindle shaped aggregate indicating constriction between the fragments as the distance between fragments increased and the matrix material flowed into the waist area. The orientation of the fractures may be either perpendicular to the extension direction or oblique to it. Control of this orientation seems to be crystallographic in some cases, the fractures being parallel to twin planes or visible cleavage planes in the porphyroclasts. Where the planes of separation appear to be crystallographically controlled (ie. parallel to twins or cleavages) and the porphyroclast was originally elongate and oblique to the greatest principal stretch then oblique separation and consequent rotation of one or more of the separated segments occurs.

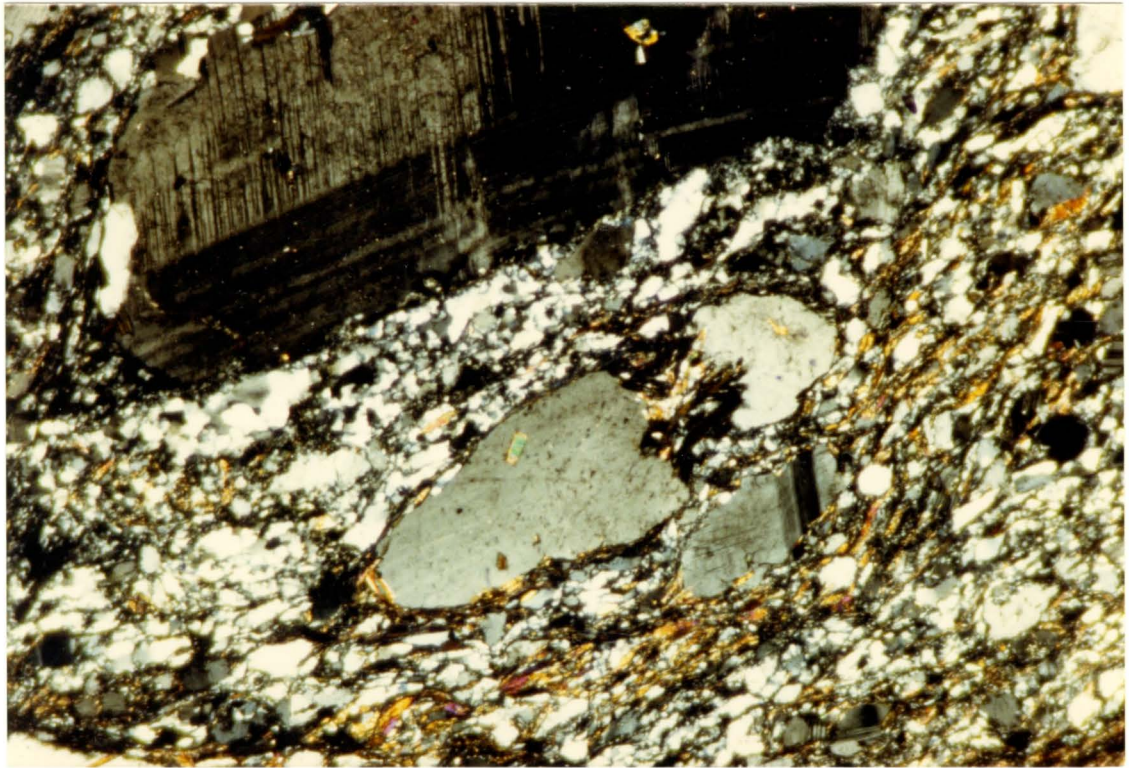
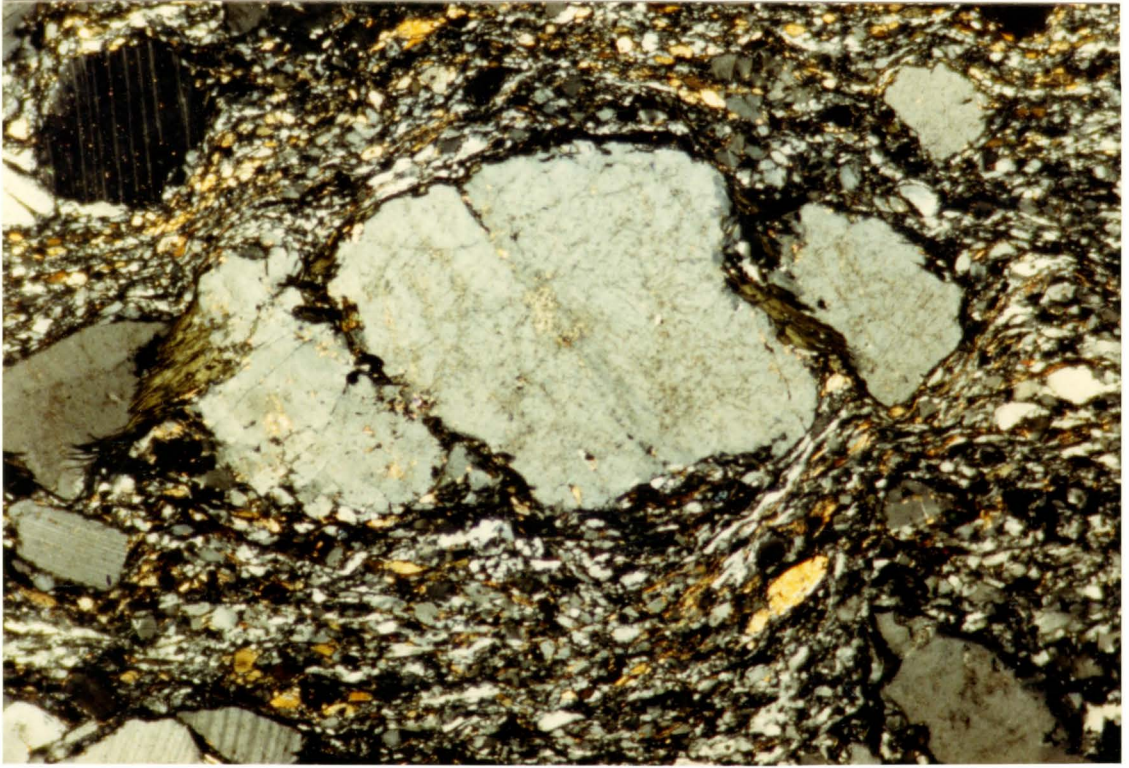
Fractures or microfaults in the feldspar porphyroclasts are also common. These features are most prominent in oblate porphyroclasts whose long axes are at low angles to the foliation and in thin sections cut subperpendicular to the stretching lineation (Table 3). These shear fractures do



Figure 16a. Feldspar pull apart showing chlorite mimicing direction of separation of fragments. An incipient fracture is visible in the large central fragment. Asymmetrical separation of fragments gives a "right lateral shear". Thin section subparallel to  $L_s$ . Field of view 2.5 mm by 4.0 mm, 240x magnification, t/s SMA-01-N.

Figure 16b. Smaller feldspar pull apart with recrystallized quartz, feldspar, biotite and chlorite in area between fragments. Larger porphyroclast at top showing dense deformation twinning and asymmetrical tail at far left. Field of view 2.5 mm by 4.0 mm, 240x magnification, t/s SMA-01-T-B.







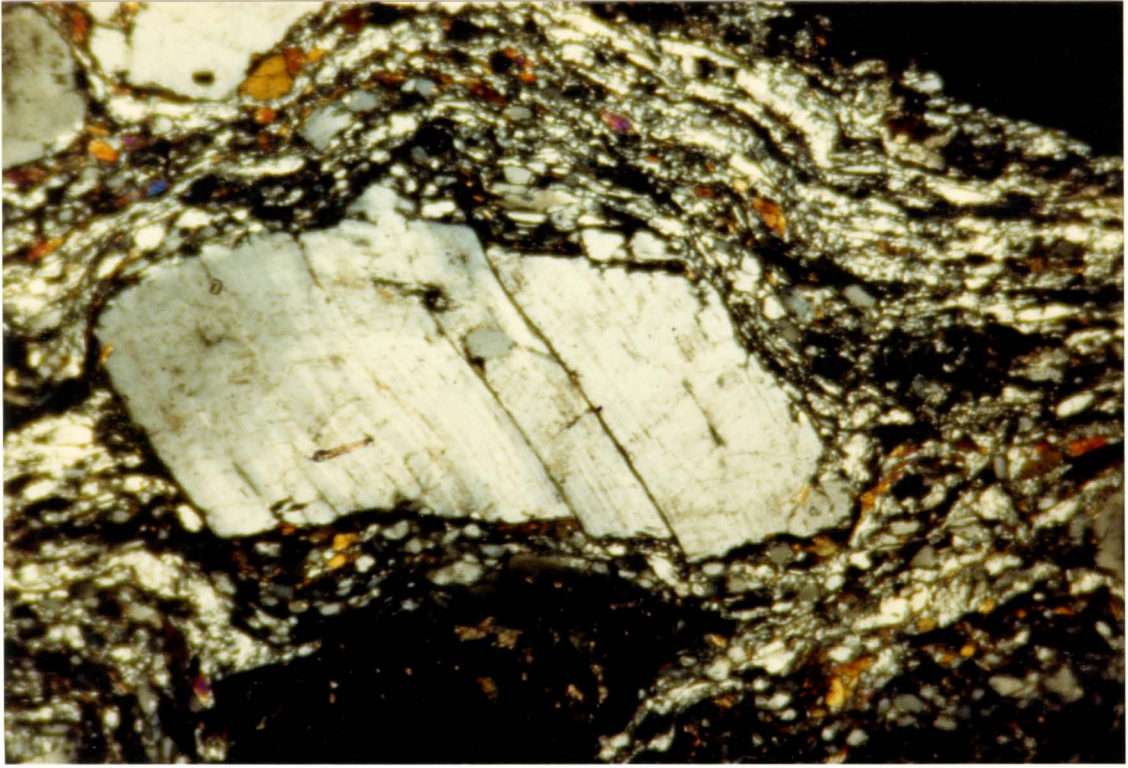
not show any significant amounts of displacement perpendicular to the shear fracture walls and therefore lack the wide in-fills of recrystallized chlorite characteristic of the tensile pull apart fractures. The fault planes are marked by narrow zones of recrystallized, fine grained chlorite, muscovite, feldspar or quartz (Figure 17b). The faults commonly lie along preferred crystallographic planes such as cleavages or twin planes as mentioned above and the fragments often contain small discontinuous fractures parallel to the major microfaults (Figure 17b). Where movement along these microfaults is large enough to result in significant amounts of strain, the boundaries of the porphyroclasts have been offset in a step-like manner (Figure 17b).

The fractures in the feldspar porphyroclasts tend to form in two principal orientations with respect to the foliation and sense of bulk shear. The first are sympathetic fractures on which the sense of shear is the same as that along C-surfaces and the bulk shear (ie. dextral) although the fracture planes are oriented at high angles in clockwise direction to the foliation plane (Figure 17a). Subsequent displacement along these planes results in a back rotation of the fractured segments in a sense opposite to that of the bulk shear. These surfaces are presumed to have formed initially as shear fractures (White et al., 1982). The second set is composed of antithetic fractures on which the sense of

Figure 17a. Sympathetic fractures in a feldspar porphyroclast. Note fractures are confined to twin planes which are bent. Fracture planes are marked by chlorite. Field of view 2.5 mm by 4.0 mm, 240x magnification, t/s SMA-01-T(A).

Figure 17b. Antithetic fractures in a feldspar porphyroclast. Fractures are parallel to cleavage or twin plane and are filled with recrystallized chlorite and quartz/feldspar. Field of view 2.5 mm by 4.0 mm, 240x magnification, t/s SMA-01-T(A).







displacement are opposite to that of the bulk shear along planes oriented at high angles in a counterclockwise direction to the foliation plane (Figure 17b). Displacement along these planes results in a rotation of the fractured segments in the same sense as that of the bulk shear. Fractures of this type are presumed to have formed initially as tensile fractures (White et al., 1982).

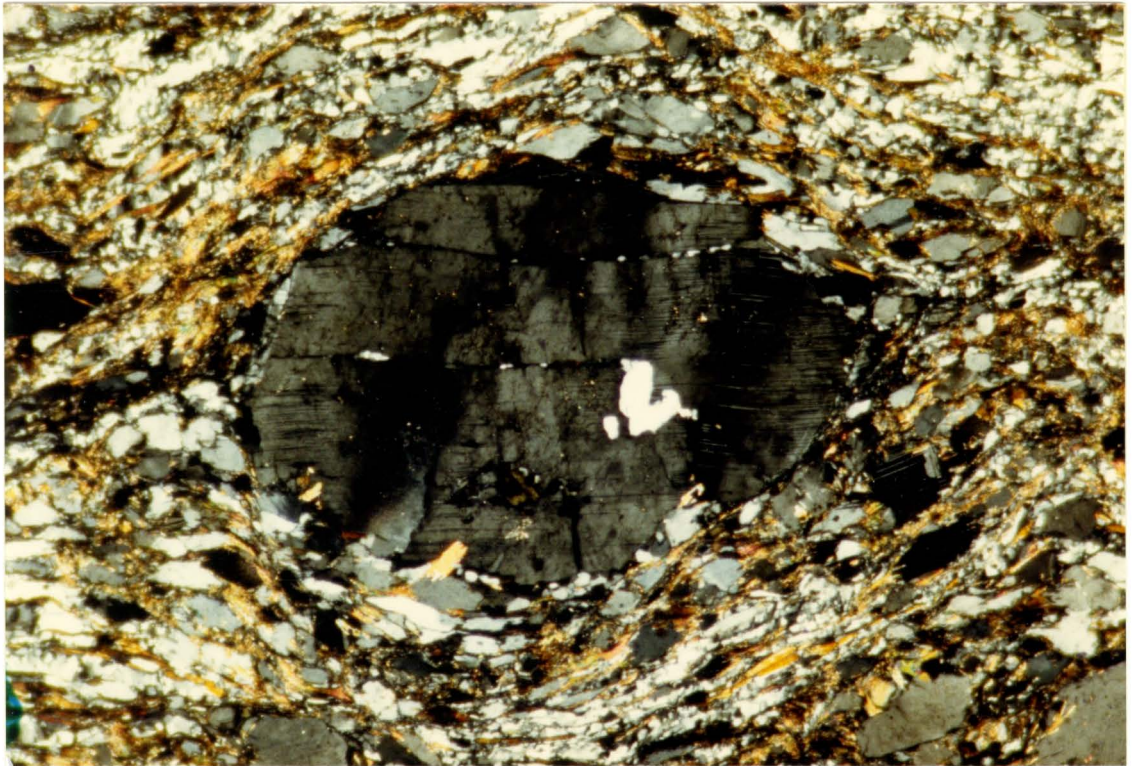
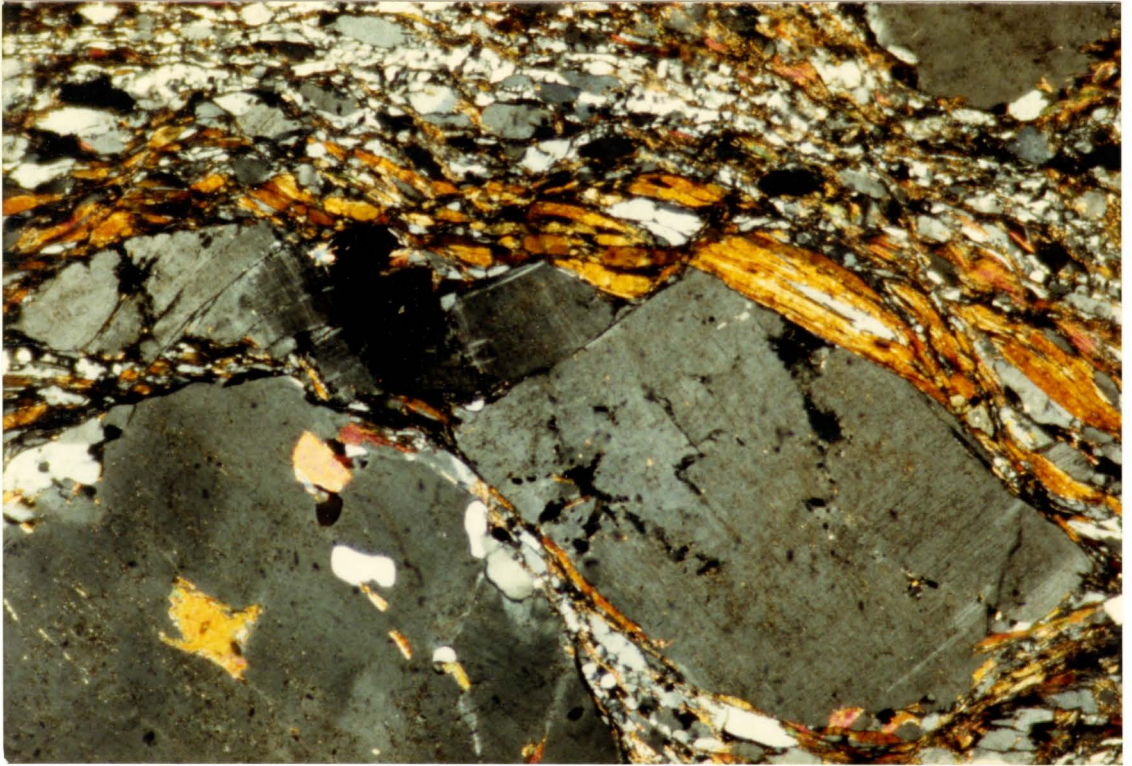
In some places porphyroclasts show strained extinction and bent deformation twins that are now cut by and displaced by microfaults. In other places porphyroclasts show bent fragments and fault planes (Figure 18). The former indicates a period of ductile deformation prior to microfaulting while the latter indicates a period of ductile deformation concomitant with or later than microfaulting.

Other ductile deformation features are also observed in the feldspars such as undulatory extinction, deformation twins, and kink bands. These features form by intracrystalline glide processes. Undulatory extinction is visible in most feldspar porphyroclasts and often accompanies other deformation features such as twinning. Extinction patterns are normally continuous across fault planes indicating they predate brittle fracturing (Figure 19). Undulatory extinction is due to intracrystalline glide which causes a misfit in the feldspar structure. Deformation twins are concentrated around the edges of some feldspar porphyroclasts and in some places taper to points or end abruptly within a grain (Figure



Figure 18. Feldspar porphyroclast that has been antithetically fractured. Interference by the large round porphyroclast has caused the fragments to bend producing strained extinction. Amphiboles adjacent to the top edge of the porphyroclast have also been fractured. Field of view 2.4 mm by 4.0 mm, 240x magnification, t/s SMA-01-S(A).

Figure 19. Undulatory extinction in feldspar porphyroclast that is continuous across fracture planes. Field of view 2.4 mm by 4.0 mm, 240x magnification, t/s SMA-01-S(A).





21). These twins may also be bent and in some instances have formed sigmoidal patterns (Figure 20a). The twins predate shear fractures, being offset by and sometimes bent with the fracture planes. Kink bands form in feldspars when twins abruptly bend into and out of a zone of twinning oriented at an angle to those in the rest of the grain (Figure 20b). This produces a band within the grain which becomes extinct at a different angle than the rest of the grain. Kinking may have occurred prior to or after fracturing in some grains.

Asymmetric porphyroclast tails are common in many sections. The tails extend away from the mantle of recrystallized mica and/or chlorite and/or quartz around the porphyroclast in long lines displaced perpendicularly away from a line through the centre of the porphyroclast and parallel to the foliation (Figure 21). These tails are part of a system similar to the  $(\sigma)_a$ -type porphyroclast system described by Passchier and Simpson (1986). In this system the main foliation is uniform except in a small distorted zone adjacent to the porphyroclast where the foliation gradually changes orientation to become roughly parallel to the porphyroclast margins. The tails in the rocks of the study area are a reaction softened material produced by degradation of the parent feldspar to mica plus quartz. The tails on either side of these porphyroclasts "step up" from the left to the right side of the foliation indicating right lateral shear (Simpson, 1986; Passchier and Simpson, 1986). The "step

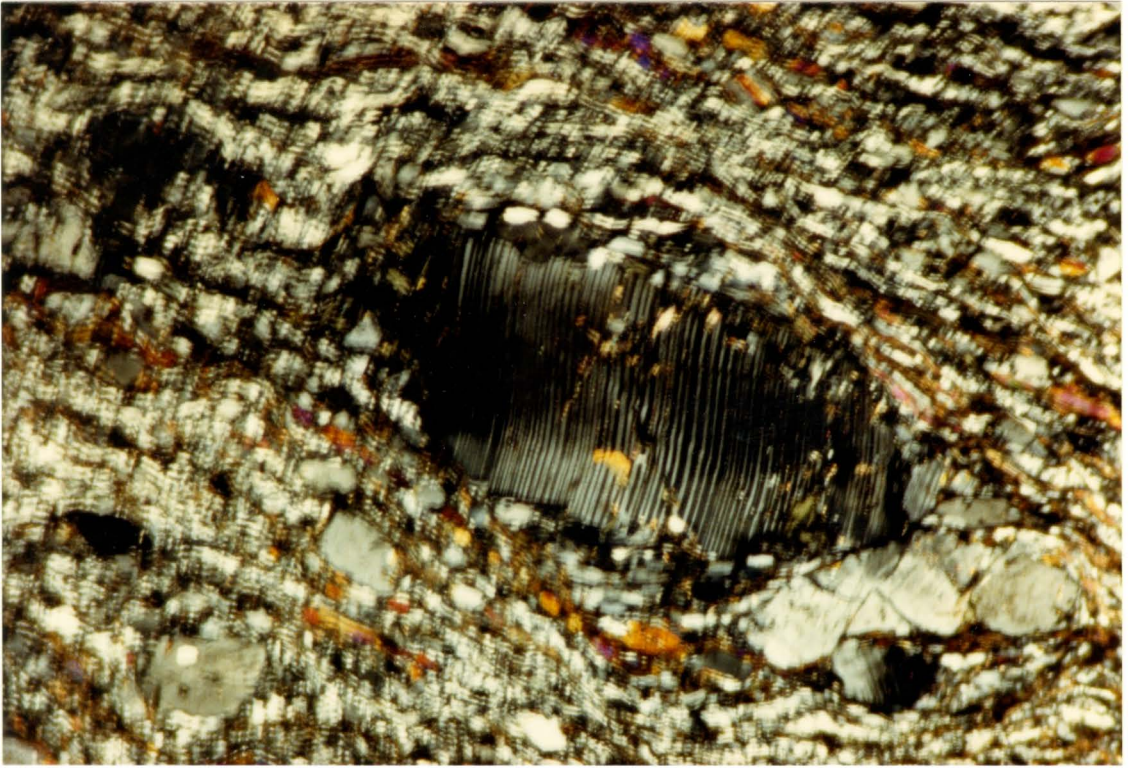
Figure 20a.

Sigmoidal deformation twins in a feldspar porphyroclast. A kink band is also visible cutting across the centre of the grain. Field of view 2.4 mm by 4.0 mm, 240x magnification, t/s SMA-01-T(A).

Figure 20b.

Well developed kink band in a deformation twinned feldspar porphyroclast. Field of view 1.0 mm by 1.5 mm, 630x magnification, t/s SMA-010-S(A).







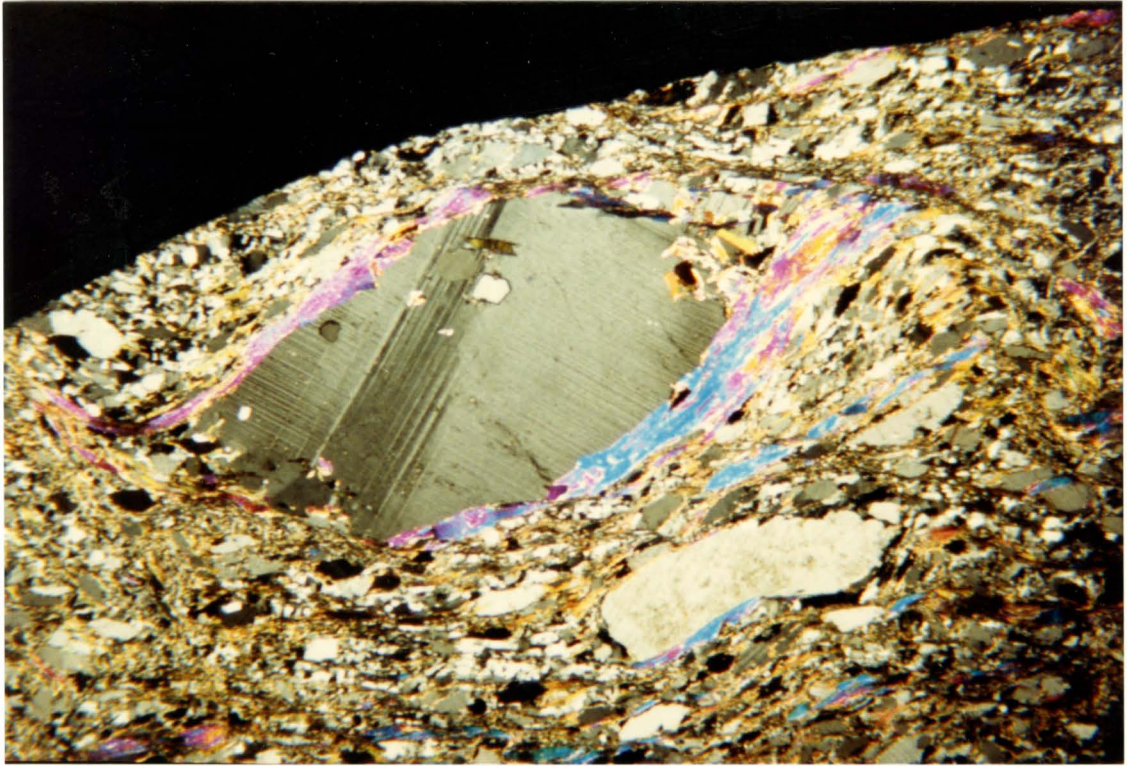
up" of the tails is often interfered with by adjacent porphyroclasts so only those porphyroclasts with asymmetrical tails isolated in relatively porphyroclast-free areas were used as kinematic indicators. The porphyroclasts displaying this texture are also normally asymmetrical in shape and often have elongate shapes oriented at low angles to the foliation in an anti-clockwise sense (Figure 21).

The ends of the porphyroclasts perpendicular to the foliation commonly display a gap filled with recrystallized material or material "plucked" from the ends of the porphs. These textures are described by Stauffer (1970) as gradational stages between two "end members". The end members are strain shadows composed entirely of recrystallized material and goatees composed entirely of deformed original material mixed with plucked fragments. The plucking probably occurs as the result of relatively high intergranular cohesion (Stauffer, 1970) and brittle behaviour of the mineral grains involved.

Some thin sections show aggregates of irregular grains of feldspar, quartz, muscovite and/or biotite and/or chlorite and/or epidote which appear to be pseudomorphs of the original porphyroclast and probably represent replacement of an original fractured and brecciated grain. Aggregates of highly fractured, disrupted feldspars appear to be partially recrystallized and contain small, relatively unstrained grains of quartz and feldspar with the relict porphyroclast



Figure 21. Asymmetric porphyroblast tails formed at the ends of a deformation twinned feldspar porphyroblast in a mica-rich rock. Note the enlarged mantle of recrystallized muscovite. The tails curve into and join with C-surfaces at upper right. Field of view 4.0 mm by 6.0 mm, 148x magnification, t/s SMA-02-D.





boundaries made visible by the thin mantle of grain boundary parallel mica flakes.

Quartz grains in the study area occur in elongated quartz ribbons whose long axes lie in and partially define the foliation. Vein-like aggregates are also present. They are continuous along the length of the thin section and are everywhere parallel to the foliation planes. The smaller quartz ribbons are less continuous than the veins and range from 2.0 mm long in the coarser grained rocks to 0.3 mm in the finer grained rocks. These ribbons probably represent stretched quartz grains of the parent migmatite. The ribbon boundaries are smooth and are defined by thin seams of fine-grained mica and/or chlorite (Figures 22 & 23). In porphyroclast-free areas the ribbons are nearly flat sided. Where they extend into areas of higher strain concentrations (ie. around porphyroclasts) they conform to the outlines of the more rigid grains, plastically deforming and wrapping around them without brittle fracturing or other discontinuities.

A secondary subgrain foliation is well developed within all ribbons and veins. The alignments of these families of oriented subgrains are best observed with the gypsum (first order retardation) plate inserted. Most subgrains are highly strained showing waves of extinction that sweep over the grains through stage rotations of up to  $25^{\circ}$ . The subgrains are elongated in one of two principal manners depending on

the thin section orientation with respect to the stretching lineation ( $L_S$ ). In thin sections oriented perpendicular to  $L_S$ , subgrains are oriented at angles ranging from  $45^\circ$  to  $90^\circ$  (mean approximately  $65^\circ$ ) to the long axes of the ribbons in an anti-clockwise sense (Figure 22a). The ribbons are normally no more than two subgrains wide. Subgrain boundaries are generally serrated and many of the boundaries contain tiny, equant recrystallized grains. The aspect ratios of ribbons in these sections range from 5:1 to 10:1 while subgrain aspect ratios range from 2:1 to 3:1. Quartz veins in these sections nearly perpendicular to  $L_S$ , are often several subgrains wide and show a more consistent obliquity of subgrains than in the ribbons in the same sections (Figure 22b). Subgrain boundaries in the veins are more recrystallized than those in the ribbons and in places the recrystallized boundaries expand into zones consisting entirely of recrystallized 5-10 micron diameter grains. All quartz grains in these sections show strained extinction and the extinction patterns trend subperpendicular to the long axis of the ribbons.

In thin sections oriented subparallel to  $L_S$  the ribbons have aspect ratios ranging from 5:1 to 10:1. The subgrains in these sections however are oriented subparallel to the length of the ribbons (Figure 23a). Subgrain aspect ratios are generally lower (near 2:1) but may be as high as 10:1. Veins are several subgrains wide while the smaller ribbons rarely



Figure 22a. Quartz subgrain fabric developed in quartz ribbons. The long axes of the sub-grains tilt in the direction of shear (ie. right) except near centre where interference from the porphyroclast at upper right has produced the opposite sense of tilt. Field of view 2.5 mm by 4.0 mm, 240x magnification, t/s sub-perpendicular to  $L_s$ , t/s SMA-01-U(A).

Figure 22b. Very well developed secondary subgrain foliation in a quartz vein. The long axes of the subgrains are tilted in the direction of shear. Field of view 2.5 mm by 4.0 mm, 240x magnification, t/s sub-perpendicular to  $L_s$ , t/s SMA-01-U(B).



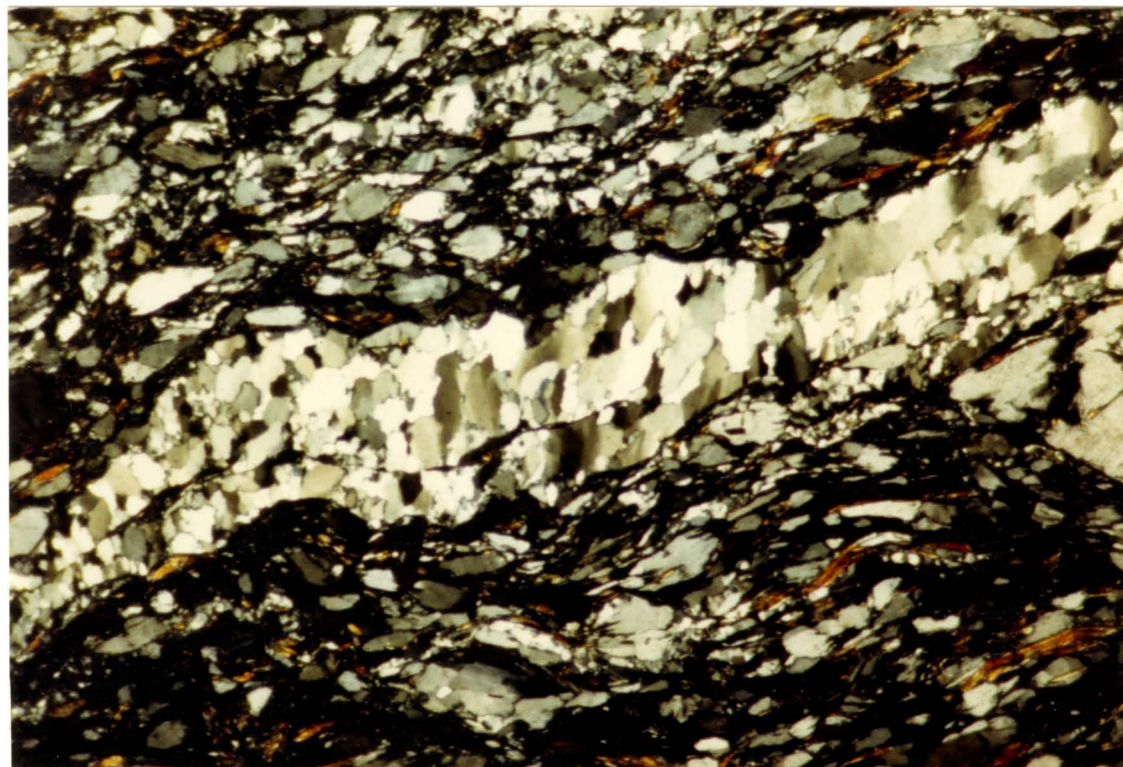
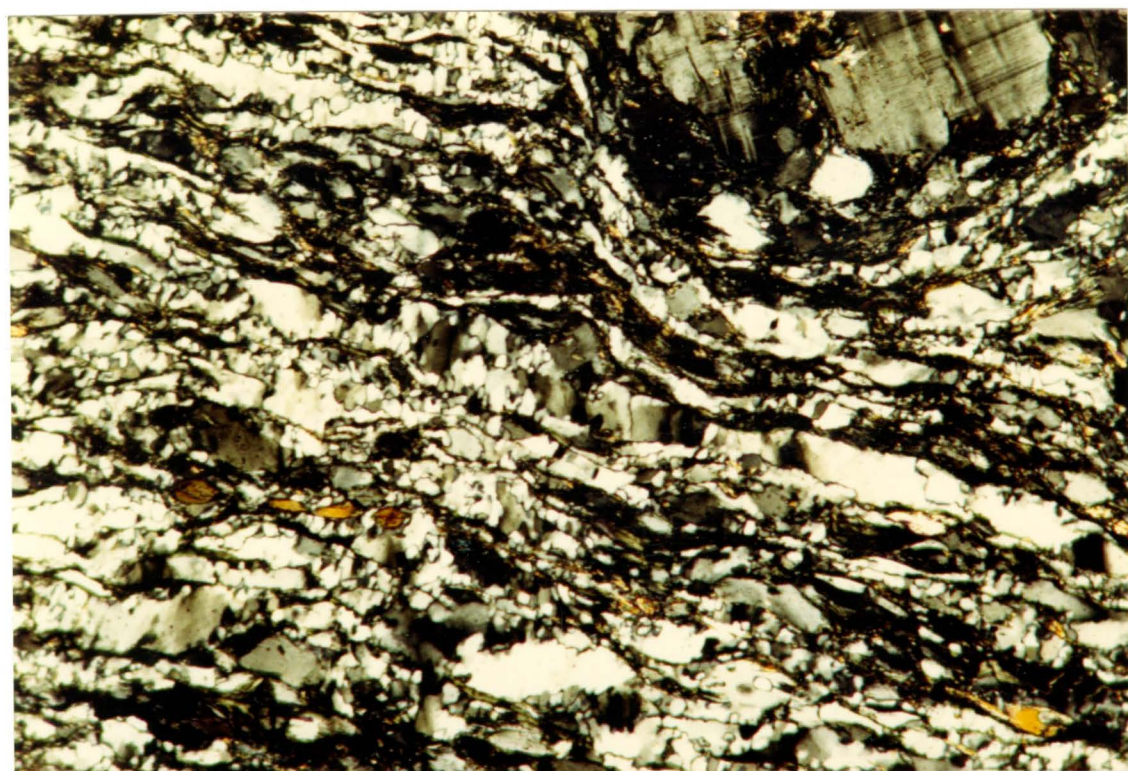
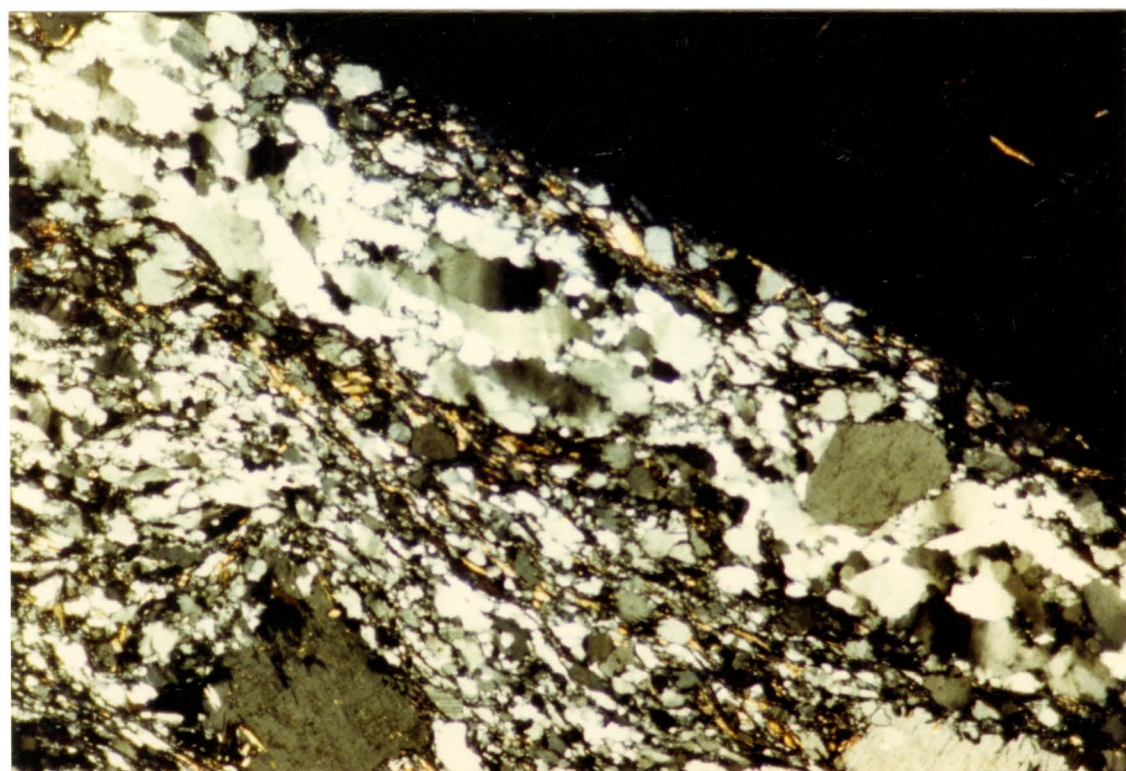
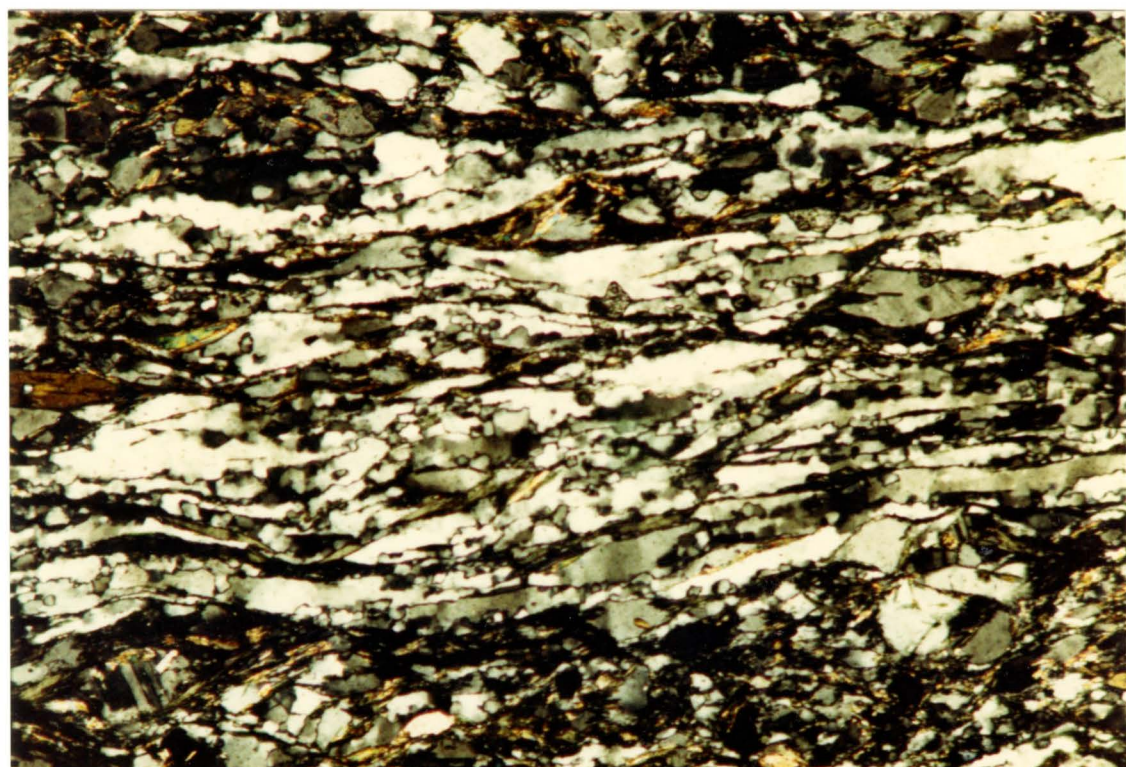




Figure 23a. A secondary subgrain foliation in quartz ribbons. Subgrains are parallel to the ribbon length. Many subgrain boundaries show polygonal recrystallized grains. Field of view 2.4 mm by 4.0 mm, 240x magnification, t/s subparallel to  $L_s$ , t/s SMA-01-U(B).

Figure 23b. A secondary subgrain foliation in a quartz vein. Many subgrain boundaries are marked by recrystallized grains. A totally recrystallized grain is visible to the right of centre. Field of view 2.5 mm by 4.0 mm, 240x magnification, t/s subparallel to  $L_s$ , t/s SMA-01-U(B).





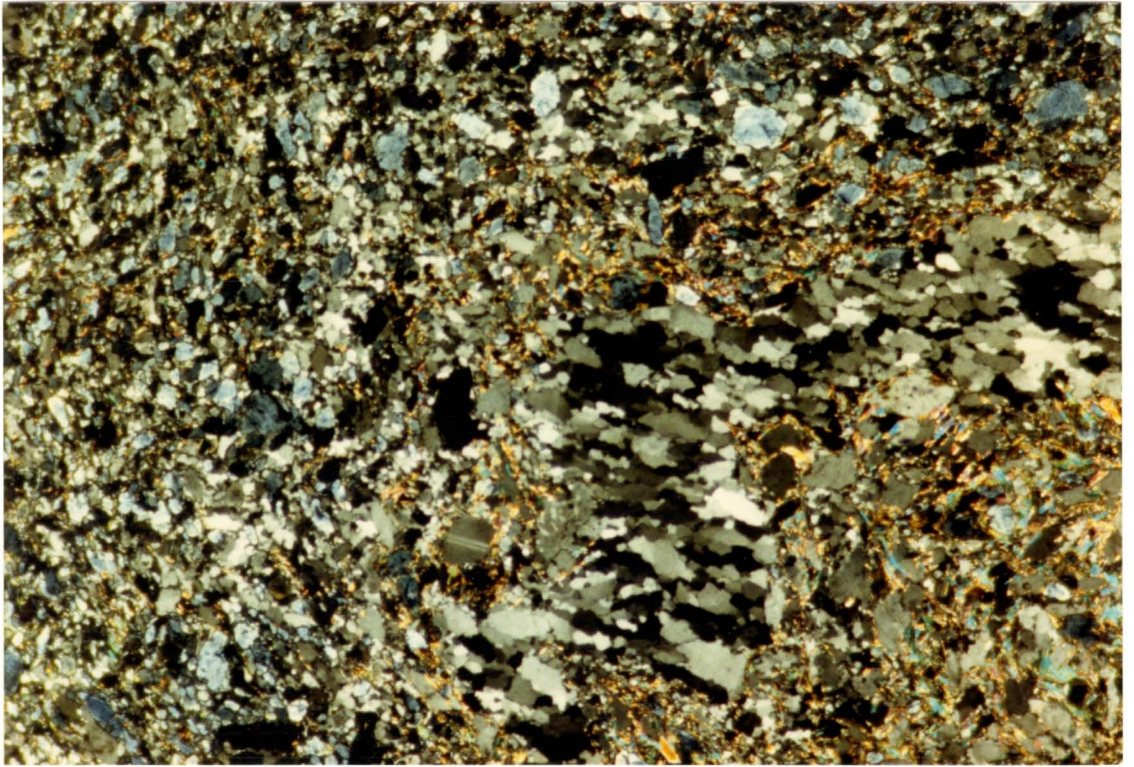
are more than two or three subgrains wide. Subgrain boundaries are again very serrated. As in the sections perpendicular to  $L_s$ , the recrystallized subgrain boundaries expand into the cores of some subgrains totally consuming the subgrain and creating sectors composed entirely of 5-10 micron recrystallized grains. The subgrains in the veins are much larger (0.2-0.5 mm lengths) compared to those in the ribbons (0.05-0.10 mm lengths) (Figure 23b). All subgrains in these sections show strained extinction and the extinction patterns trend parallel to the ribbon and subgrain boundaries, sweeping across the width of the subgrains upon stage rotation.

In thin sections hosting folded quartz veins, the subgrains have aspect ratios of 3:1 or 4:1 and the long axes of the subgrains are oriented subparallel to the axial plane of the folds, especially in the more tightly folded limb and hinge areas (Figure 24). In these areas the aspect ratios are highest and approach 6:1 in places.

The kinematic indicators described above are discussed in detail along with their kinematic and rheological significance in chapter 4.

Figure 24. Axial planar parallel subgrain foliation in folded quartz vein. Degree of recrystallization is very low. Note the clinozoisite (blue) dominant at the left. Field of view 2.5 mm by 4.0 mm, 240x magnification, t/s SMA-01-O(B).





## Chapter 4: Discussion

### Introduction

The development of shear zones is commonly viewed as resulting from progressive simple shear. During ideal progressive simple shear, shear strain within the shear zone rises and consequent rotations cause any previously randomly oriented lines or planes within the shear zone to be progressively rotated into near parallelism with the shear zone boundaries. At a point, shear strain becomes so high that it is no longer possible to distinguish lines or planes previously oriented oblique to the shear zone walls (eg. migmatite layering in the "protolith") from the mylonite layering. These rotations correspond to rotation of the principal finite strain axes. The instantaneous principal strain or kinematic axes remain fixed however so the deformation is non-coaxial. Although it is a simplification of flow in rocks, "kinematic indicators" may be defined as structures whose asymmetry and/or rotational behaviour during progressive deformation reflect the rotation of the finite principal strain axes with respect to the instantaneous principal strain axes and/or shear plane (Hanmer, 1984).



## Strain Estimate

An estimate of minimum shear strain in the study area may be made if it is first assumed that the maximum obliquity (ALPHA) of any original migmatitic layering in the parent migmatite was  $90^\circ$  to the shear zone boundary. Mylonitic layering now varies by a maximum of  $5^\circ$  on either side of the mean foliation. Regional trends indicate that the mean foliation is approximately parallel to the shear zone (ie. "straight zone") boundaries. If the new position (ALPHA') of migmatitic layering is at  $5^\circ$  to the shear zone walls, a value of shear strain (GAMMA) may be calculated as below (Ramsay & Hubber, 1980).

$$\cot (\text{ALPHA}') = \cot (\text{ALPHA}) - \text{GAMMA}$$

$$\text{ALPHA}' = 5^\circ$$

$$\text{ALPHA} = 90^\circ$$

$$\text{GAMMA} = 11$$

If the above assumptions are correct, then a minimum shear strain of 11 can be assigned to the rocks of the study area. This estimate is a gross over simplification of the true strain state. It does however, give a reasonable minimum value of shear strain and helps characterize the strain involved in formation of the mylonite in the study area.

## Mesostructures and Microstructures: Foliation and Lineation

The foliation or "S-surfaces" (after Berthe et al., 1979) in the study area formed as the result of accumulation of finite strain in the rocks and are by definition parallel to the XY plane of the finite strain ellipsoid (Ramsay and Graham, 1970). But it has already been demonstrated that in the study area, shear has taken place in the foliation plane. This suggests that the XY plane of the finite strain ellipsoid is slightly oblique to the foliation plane (Figures 25 & 26).

The steeply plunging lineation in these rocks is recognized as both a stretching lineation and a corrugation lineation. The stretching lineation ( $L_S$ ) indicates a significant component of subvertical extension, while the corrugation lineation indicates a subhorizontal component of compressive shear. The stretching lineation therefore must be sub-parallel to the  $X_f$  strain axes and the corrugation lineation must be sub-perpendicular to the  $Y_f$  strain axes of the finite strain ellipsoid (Figure 25).

The stretching lineation would thus suggest a subvertical component of extension that is best explained by vertical motions in the shear zone. The corrugation lineation on the other hand, suggests a horizontal component of compressive shear that is best explained by horizontal motions within the shear zone. Regional metamorphic and structural data from



the Artillery Lake area indicate domains to the west represent increasingly deeper exposures of structural levels. This suggests some vertical motion along the domain boundaries and that motion was "east side up". The stretching lineation may therefore be due to subvertical extensions within the straight zone rocks. The corrugation lineation and other data from the study area and from other localities within the straight zone also indicate significant horizontal motion within the study area. The corrugation lineation probably formed due to compressive right lateral shear stresses that caused a "crinkling" of the foliation. These two motions are inherently incompatible if the two expressions of the lineations formed during the same episode of deformation. From all information available however, both the folding and extension occurred coevally. An alternative model for the synchronous formation of both "lineations" is therefore needed and is discussed below.

### Feldspar Porphyroclasts

Feldspar porphyroclasts and their related structures are some of the most useful kinematic indicators observable in thin section and partially clarify the dilemma mentioned above. In thin sections oriented sub-perpendicular to  $L_S$ , asymmetrical porphyroclast tails are common. These porphyroclast tails were described in chapter 2 and are similar to those "tails" in the  $(\sigma)_a$ -type porphyroclast system

described by Passchier and Simpson (1986). These  $(\sigma)_a$ -type porphyroclast systems are thought to develop when the rate of dynamic recrystallization of the porphyroclast is high with respect to the shear strain rate in the rock. The deformation accompanying formation of these porphyroclast systems involves non-coaxial flow which imparts a spinning motion on the rigid porphyroclasts (Freeman, 1985 fide Passchier and Simpson, 1986). The flow in the matrix may produce foliation elements that interfere with the rotating porphyroclast in a complex way. The resulting structure therefore contains information on the flow regime and the deformation path in the volume of rock surrounding the porphyroclast. The tails on the porphyroclasts are these "resulting structures" and their asymmetry provides kinematic information indicating right lateral shear.

The actual 'genesis' of the sigma-type porphyroclast system is dependent mainly on the recrystallization rate per shear strain rate as described by Passchier and Simpson (1986). Other factors such as finite shear strain and porphyroclast shape are also discussed by Passchier and Simpson (1986) but a full discussion of these factors is beyond the scope of this study.

If the axis of rotation of the porphyroclasts is assumed to be sub-parallel to  $L_s$ , then the extensional pull-aparts could have originated by a mechanism other than extension due to subvertical motions associated with the straight zone



displacement. The rolling of the feldspars between foliation planes produces a real but "passive extension" perpendicular to the lateral shear motion vectors but in the foliation plane (Figure 25). In a similar situation, Lister and Price (1978) suggest that extremely heterogeneous strains would develop around the rotating porphyroclast and that extension parallel to the rotation axis would also be aided by vortex motions in the surrounding material. The feldspar pull aparts in the study area may therefore be attributed to a component of extension oriented parallel to the greatest finite strain axes,  $X_f$  and directly resulting from large lateral shear displacements. This passive extension can easily be modelled by rolling a piece of plasticine between two pieces of plywood. The plasticine will undergo extension perpendicular to the shearing direction producing a cigar shaped mass.

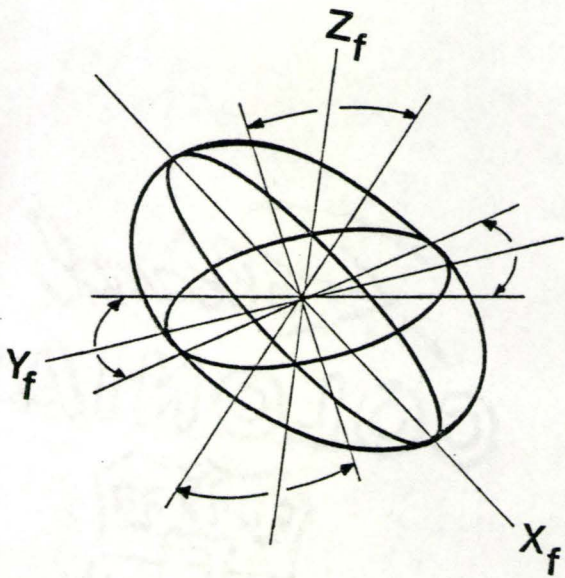
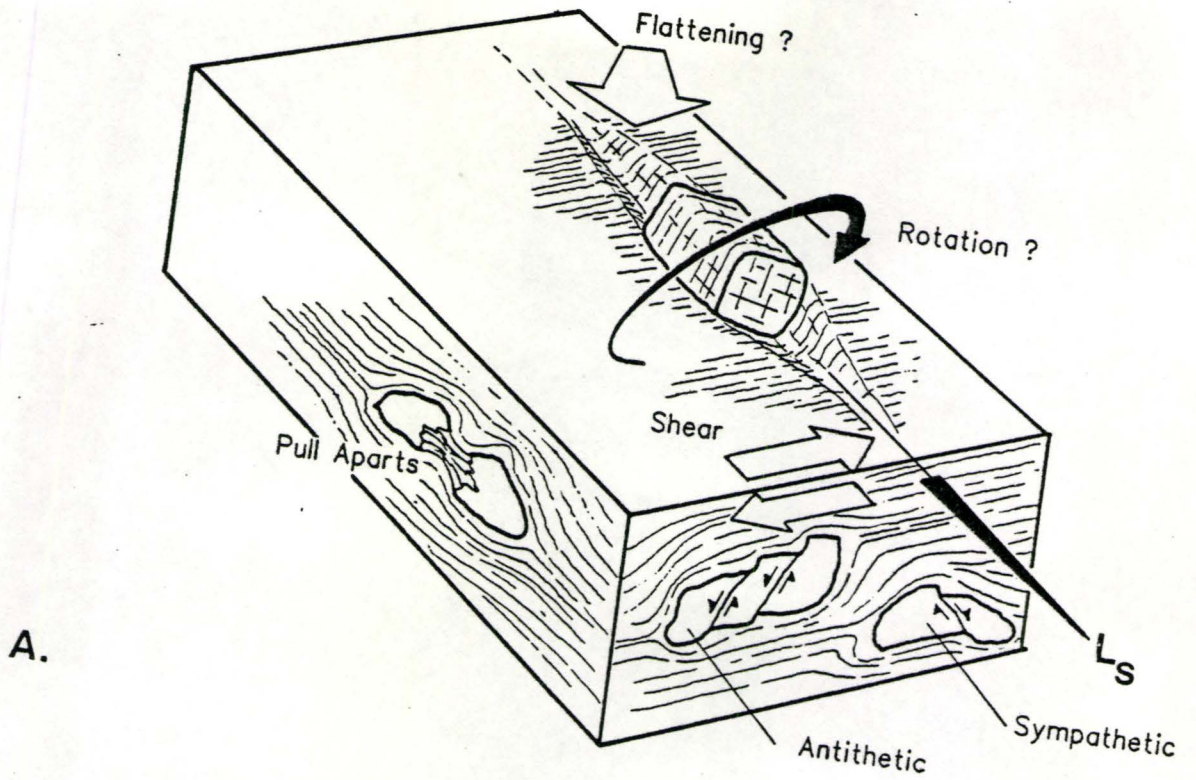
Another feature which supports the rolling feldspar interpretation (ie. dominantly lateral shear) is a roughly symmetric distribution of mica (biotite) flakes in thin sections parallel to the foliation. The flakes of biotite are preferentially oriented at angles of  $40^\circ$ - $60^\circ$  to vertical ( $20^\circ$ - $40^\circ$  to  $L_s$ ) and plunge to the northeast. This angle deviates significantly from the stretch and the corrugation lineation. This feature contradicts the notion that the majority of the strain was restricted to the X direction. Instead, it suggests a significant pure shear component

Figure 25.

A. Block diagram showing geometric relationship of feldspar porphyroclast textures. Right lateral shear produces a rotation of the porphyroclasts between foliation planes. Extensional pull aparts are parallel to the stretching lineation ( $L_s$ ). Sympathetic and antithetic micro-faulted feldspar porphyroclasts are viewed in sections perpendicular to  $L_s$ .

B. Strain ellipsoid showing prinipal strains and their positions relative to the block diagram.





acting in the Y direction which has oriented mica flakes in that direction (O'Donnel, 1986).

One problem does arise from this model. If the lineation is the axis of rotation of the rolling porphyroclasts, then it must be perpendicular to the flow (shear) vectors. The lineation plunges approximately  $70^{\circ}$  to the northeast so that shear motion vectors of right lateral sense would plunge approximately  $20^{\circ}$  to the southwest and would produce a "west side up" displacement. This is inconsistent with data from regional mapping but could be explained by local reversals in flow direction possibly due to the readjustments after initial shearing had ceased. The importance of this model is that it is kinematically consistent. That is, both stretching in a vertical sense, and shear in a horizontal sense may arise from this model.

Both shear fractures and pull aparts occur predominantly in oblate to elongate porphyroclasts with the fractures oriented sub-perpendicular to the long axes of these porphyroclasts. This shape control of fracturing in the porphyroclasts indicates that a "fibre loading" mechanism is operating (Wakefield, 1977).

Antithetically and sympathetically fractured porphyroclasts formed at the same time as the pull apart porphyroclasts. These porphyroclasts are observed in the same thin section (perpendicular to  $L_s$ ) as the rotated porphyroclasts with asymmetrical tails. The fracturing of these



porphyroclasts, however, accommodates not only a rotational component but also an extensional component. The bimodal distribution of antithetic and sympathetic fractures is a function only of the preferred orientation of crystallographic planes within the grains. The sympathetic fractures formed only in porphyroclasts with a crystallographic plane (twin or cleavage plane) originally oriented at angles close to the orientation of C-surfaces. This direction is also sub-parallel to the principal shortening ( $Z_f$ ) direction and therefore these fractures originated as shear fractures (Figure 25). Antithetic fractures are oriented nearly perpendicular to the sympathetic fractures. Again these fractures form only in grains with a crystallographic plane originally oriented at angles nearly perpendicular to the principal shortening ( $Z_f$ ) direction (Figure 25). These fractures are thought to originate as tensile fractures. Continued deformation along fracture planes in the antithetically and sympathetically fractured grains allows the grain to extend in the direction of flow. Continued displacement is also accompanied by body rotations of the fragments in both types. Sense of rotation in the in the antithetically fractured grains is in the same sense as flow in the rock (ie. clockwise) and in the opposite sense in the sympathetically fractured grains (ie. anti-clockwise).

Internal features of the porphyroclasts also provide kinematic information. Undulatory extinction, deformation

twins and kink bands form by ductile intracrystalline glide processes. This occurs under amphibolite grade conditions in feldspars. In the study area, such features are cut by brittle tensile pull aparts and shear fractures and therefore indicate a period of ductile deformation prior to the brittle shear and tensile pull apart fracturing.

### Extensional Shear Surfaces and Mica "Fish"

"Shear bands", or what may be generically referred to as "extensional shear surfaces", are observed at both mesoscopic and microscopic scale in the study area. These features have been described by various researchers (eg. Berthe et al., 1979; Platt and Vissers, 1980; Lister and Snoke, 1984) and given different names but from here on will be referred to as "C-surfaces" after Berthe (1979). It is generally agreed that these C-surfaces are displacement discontinuities as well as the loci of zones of intense shear strain developed during flow. The S-surfaces and C-surfaces together often form what is called a "C and S fabric". The recognition of C and S fabric allows assertion of a statement that, intense non-coaxial laminar flow has taken place. It also allows, at least locally, the orientation of the bulk shear plane and the direction of shear to be estimated (Lister and Snoke, 1984). C-surfaces deflect or displace pre-existing anisotropies with a consistent sense of shear and thus provide a reliable sense of bulk shear indicated as dextral



in the rocks of the study area. C-surfaces were also observed in thin sections sub-parallel to  $L_s$  indicating vertical motions with an "east side up" sense of displacement.

Mica "fish" result from the same C-surfaces mentioned above and their recrystallized tails often define the C-surfaces. The "fish" therefore result from the same locally high shear strains which produced the C and S fabric. The 001 cleavage planes of the "fish" are often back rotated into the direction of shear so that the 001 planes lie at low angles to the mylonitic foliation and face the local incremental shortening direction ( $Z_f$ ).

Several mechanisms for the origin of "C and S fabric" (and therefore mica "fish") have been suggested. From these suggested mechanisms, two models emerge as what the author believes, are the best representations of the mechanisms which may have produced the "C and S fabric" in the rocks of the study area. The first model suggests a synchronous development of C and S-surfaces, the C-surfaces being continuously rotated into the foliation during progressive non-coaxial deformation (Platt and Vissers, 1980). The second, and in the author's mind, the more plausible model, suggests a mylonitic foliation (ie. S-surfaces) forms early in the deformation history as the result of accumulated finite strain. C-surfaces begin to form later as anisotropies develop in the fabric which may induce locally

intense shear strains. In this second model, the C-surfaces are merely later stages in the evolutionary process which also formed the S-surfaces (Lister and Snoke, 1984). The non-penetrative C-surfaces in the rocks of the study area may therefore only be the latest initial stage of many previous evolutionary processes or cycles "frozen" into the rocks. These rocks conceivably could have experienced many previous evolutionary cycles. Any evidence of the previous cycles would have been obliterated by rotation of the C-surfaces into the mylonitic foliation during continued deformation.

### Asymmetrical Folds

Asymmetrical folds in the mylonitic layering of the rocks in the study area are visible both at mesoscopic scale and microscopic scale. These folds may develop due to amplifications of local perturbations in the flow of the rocks (Simpson, 1986). Porphyroclasts also become aligned along one limb of the folds in the study area. The porphyroclasts themselves must be aligned along the limbs which are in a field of flattening. The other limb of these folds is therefore in a field of extension where layers of quartz/feldspar material have been stretched and boudinaged (Figure 10).

Both C and S fabric and asymmetrical folds have certain rheological implications attached to them. Lister and Snoke (1984) suggest two such implications. One is that local



yield phenomenon involving critical yield stresses are responsible for the development of C-surfaces. The other is that the yield stress may be passively approached by material softening rather than increased shear strain as deformation proceeds. This material softening ensures the localization of intense shear strains in narrow zones.

The asymmetrical mesofolds form only in the mica-rich rocks of the study area and are often observed to be localized around heterogeneities such as feldspar porphyroclasts. Microfolds are common in both mica-rich and mica-poor rocks. This implies not only that the folds result from perturbations in the flow caused by heterogeneities but also implies that flow characteristics vary in the mica-poor and mica-rich rocks. It is therefore immediately obvious that the rheological properties of the two rock types (mica-poor and mica-rich) vary and that flow in the mica-rich rocks was more conducive to the formation of mesofolds.

### Asymmetrical Pull Aparts

Type 1 and Type 2 asymmetrical pull aparts (cf. Hanmer, 1984) are visible in outcrops in the study area. The more lenticular Type 2 amphibolite pull aparts appear to be the result of a low competency contrast between the amphibolite and mylonitic matrix. The more angular Type 1 pull aparts appear to be the result of a higher competency contrast between the competent amphibolite and the incompetent

surrounding quartz matrix. The Type 1 pull aparts may have begun deformation in the lower competency contrast environment initially forming Type 2 pull aparts. Later, injection of the quartz vein material may have transformed the amphibolite material into a higher competency contrast environment and therefore into a different rheological environment which favoured more brittle Type 1 pull apart behaviour. In the study area, these pull aparts provide only supportive kinematic information if the bulk shear sense is already known from other more reliable indicators.

#### Secondary Quartz Subgrain Foliations

Quartz ribbons and quartz veins in the study area contain a secondary, subgrain shape, preferred orientation visible only in thin section. Subgrains are formed by dynamic recrystallization which may be accomplished by two mechanisms. Progressive rotation of subgrains during crystal plastic deformation continues until the lattice misfit exceeds  $10^\circ$  or  $15^\circ$  where a new subgrain is formed (Poirier and Nicolas, 1975; White, 1976; fide Simpson, 1986). Alternatively, recrystallization may take place by progressive migration of subgrain boundaries from less highly strained subgrains to more highly strained subgrains (White, 1976; Urai, 1985; fide Simpson, 1986). These two mechanisms combine to produce elongate new subgrains whose long axes are parallel to the incremental stretching direction.



The attitude of the oblique foliation formed by elongate subgrains will depend on the shear strain accumulated since the last recrystallization event. This is because recrystallization of quartz obliterates any previous accumulations of strain, effectively resetting the "finite strain clock" (Lister and Snoke, 1984). Simpson (1986) also cautions that these secondary foliations are reliable indicators of the sense of shear for only the last increment of deformation since they are easily reoriented if the mylonitic layering becomes folded as it is in the study area.

The subgrains in the study area indicate the greatest incremental stretch to be near vertical, parallel to  $L_S$  in thin sections oriented parallel to  $L_S$ . Subgrains observed in thin sections oriented sub-perpendicular to  $L_S$  indicate intermediate incremental stretch to be at a mean of  $64^\circ$  to the foliation in an anti-clockwise sense. These subgrain fabrics may therefore indicate a final deformation increment of significant vertical motion.

#### Estimate of Strain Axes Orientations

From all the features discussed above, the approximate positions of the finite strain axes in the study area may be estimated. Features in thin sections oriented sub-parallel to  $L_S$  indicate significant stretching and shear displacements in an "east side up" sense. Features in thin sections sub-perpendicular to  $L_S$  indicate rotation of the rigid por-

phyroclasts and right lateral shear displacements. Therefore, flattening must have occurred sub-perpendicular to the shear plane (the foliation) and from the east to produce the observed dextral shear indicators. Strain axes are estimated to fall in the areas indicated in Figure 26.

The assemblage of structures observed both in thin section and in outcrop is compelling evidence supporting the idea that the stretching lineation ( $L_S$ ) represents the greatest finite strain direction ( $X_f$ ).  $X_f$  however must be at shallower angles to horizontal than  $L_S$  as is indicated by the biotite fabric in thin sections parallel to the foliation ( $S_0$  in Figure 26). Intermediate finite strain ( $Y_f$ ) is therefore at moderately low angles to the foliation but must, by definition, be perpendicular to  $X_f$ .

Brittle deformation features accompanied by sinistral displacements are present in the study area. These indicate much later brittle faulting mechanisms probably related to the Bathurst Fault tectonics and are therefore unrelated to the deformations being examined in this study.

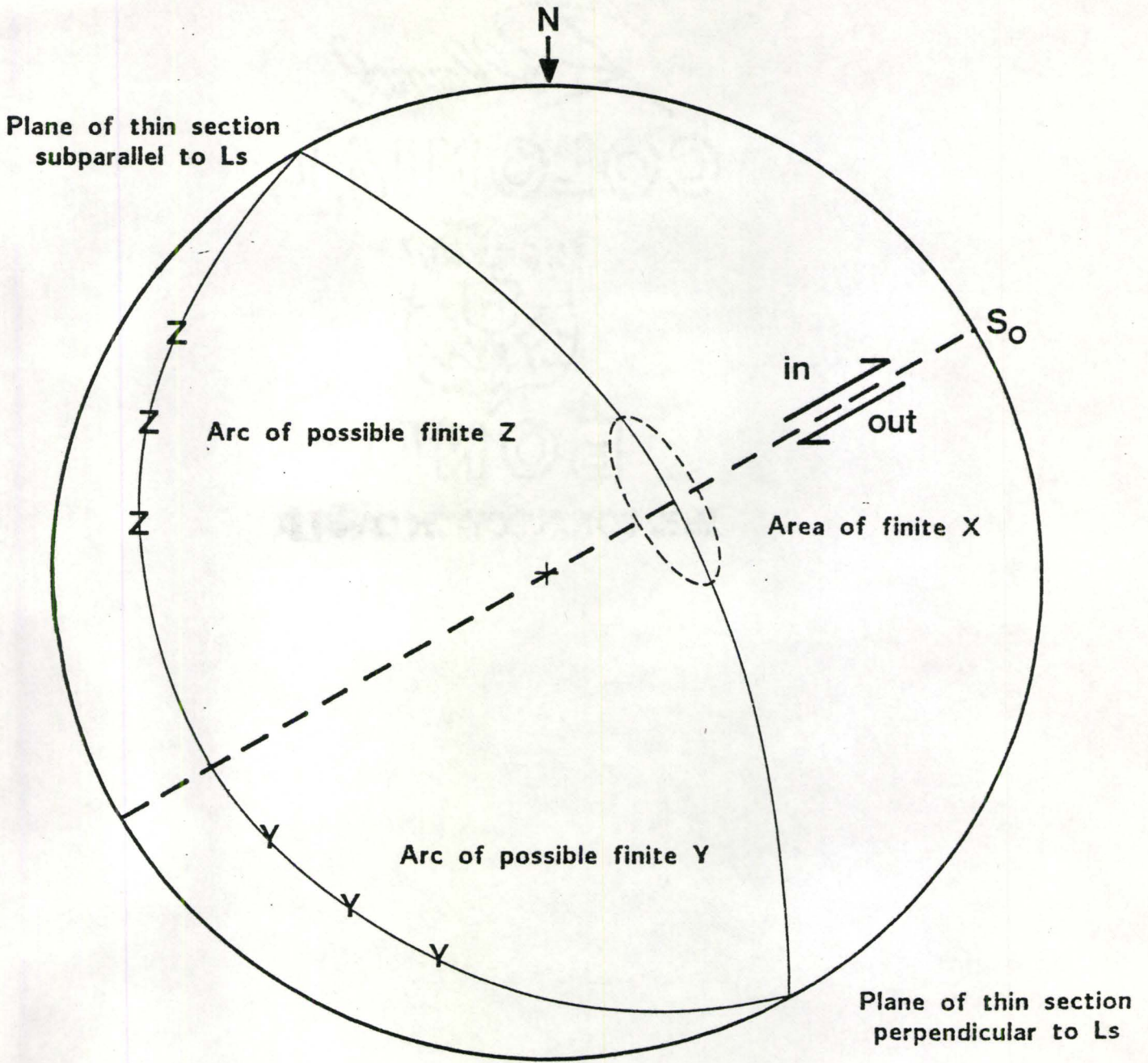
### Discussion of Metamorphism, Microstructures, Mesostructures and "The Big Picture"

Metamorphic grades in the study area have been estimated to have reached amphibolite grade both by regional mapping



Figure 26.

Stereoplot indicating possible positions of principal finite strain axes in the study are determined from thin sections perpendicular and subparallel to  $L_s$ . Shear plane is parallel to the foliation ( $S_o$ ). The position of finite X is subparallel to  $L_s$ . Finite Z marks the position of flattening. Finite Y lies close to  $S_o$  but not in it. Southeast block is upthrown (out) and northwest block is downthrown (in).





(Henderson et al., 1987) and by petrological observations made on thin sections by the author (cf. Chapter 2). Refinement of this assessment of metamorphic grade is possible if the deformation textures of certain minerals are considered in relation to their mode of deformation and metamorphic grade.

Quartz begins to deform in a ductile fashion at the onset of greenschist metamorphic conditions. Feldspars on the other hand, remain strong and display dominantly brittle deformation features into amphibolite grade conditions (Simpson, 1985; Boullier, 1980; Wakefield, 1977). Applying this information to the rocks in the study area indicates that deformation began in amphibolite grade conditions. This is indicated by ductile deformation features such as kink bands, deformation twins and strained extinction in the feldspar porphyroclasts. Deformation continued as metamorphic conditions relaxed, causing the porphyroclasts to deform in a brittle fashion. The extensional fractures in the pulled apart porphyroclast fragments indicate deformation under greenschist conditions (Boullier, 1980). The pull aparts produced a dilatation and the chlorite precipitated in these gaps indicates an ingress of fluids into the rocks. The chlorite fibers mimic the motion of the feldspar fragments so that coeval precipitation of the chlorite must have taken place.

Henderson et al. (1987) have suggested that domains to the east in the Artillery Lake map area represent exposures of deeper structural levels. This implies a significant component of vertical motion, possibly localized along domain boundaries. If deformation continued during this uplift then the rocks of the study area could have been uplifted from lower structural levels where amphibolite conditions prevailed to higher structural levels where greenschist conditions prevailed. The brittle fractures overprinting the ductile features in the porphyroclasts of the area indicate such a sequence took place. Wakefield (1977) has noted similar relationships in his study of the Lethakane shear zone.

More detailed regional scale analysis of metamorphic-structural relationships in the Artillery Lake area would confirm or disprove the sequence of events proposed above.



## Chapter 5: Conclusions

In the shear zone studied, deformation features are consistent with those normally associated with ideal simple shear. The kinematic indicators visible both in outcrop and thin section indicate dominantly right lateral shear displacements. A significant vertical component of displacement is also indicated.

The maximum principal finite strain axis in the area is subparallel to the steeply plunging stretching lineation visible in outcrop in the study area. The intermediate finite strain axis in the area is subhorizontal and subparallel to the mylonitic foliation. The direction of flattening in the study area is oblique to the mylonitic foliation and directed from the east.

Metamorphic conditions at the onset of deformation were of epidote-amphibolite facies. During continued deformation, metamorphic conditions relaxed into greenschist facies as indicated by feldspar microstructural strain features. Regional metamorphic trends in the Artillery Lake area indicate progressively deeper exposures of structural levels to the east that may suggest significant vertical motions associated with the domain boundaries. The variations in

deformation characteristics and metamorphism in the study area are consistent with the notion of significant uplift of domains to the east.

### Suggestions For Further Research

More detailed structural kinematic studies on the "straight zone" and other surface expressions of the Thelon Front in the Artillery Lake are necessary before a complete understanding of the motions involved with Thelon Front tectonics within the area can be realised.

More detailed experimental studies on the behavior of feldspars under strain at varying metamorphic conditions may also allow these features to be used in areas where metamorphic conditions changed too rapidly for mineral phases to equilibrate.



## References

**Andrews, J.R.**

- 1984: Fracture controlled feldspar shape fabrics in deformed quartzo-feldspathic rocks, J. Struct. Geol., 6, pp. 183-188.

**Berthe, D. and Brun, J.P.**

- 1980: Evolution of folds during progressive shear in the South Armorian Shear Zone, France. J. Struct. Geol., 2, pp. 127-133.

**Berthe, D., Chonkroune, P., and Jegouzo, P.**

- 1979: Orthogneiss, mylonite and non-coaxial deformation of granites; the example of the South Armorian shear zone. J. Struct. Geol., 1, pp. 31-42.

**Bostock, H.H.**

- 1987: Geology of the Taltson Lake area, south half, District of Mackenzie; in Current Research, Part A, Geological Survey of Canada Paper 87-1A, report 47.

**Boultier, A.M.**

- 1980: A preliminary study on the behavior of brittle minerals in a ductile matrix: example of zircons and feldspars, J. Struct. Geol., 2, pp. 211-217.

**Deer, W.A., Howie, R.A., and Zussman, J.**

- 1982: An Introduction To The Rock Forming Minerals, Longman Group Limited, 528 p.

**Ehlers, E.G. and Blatt, H.**

- 1982: Petrology: Igneous, Sedimentary and Metamorphic, W.H. Freeman and Company, 732 p.

**Fraser, J.A.**

- 1964: Geological Notes on Northeastern District of Mackenzie, Northwest Territories; Geological Survey of Canada, Paper 63-40.

- 1972: Artillery Lake map area, District of Mackenzie; Geological Survey of Canada, Paper 71-38, 17 p.

**Freeman, B.**

- 1985: The motion of rigid ellipsoidal particles in slow flows, Tectonophysics, 113, pp. 163-183.

Frith, R.A.

- 1982: Second preliminary report on the geology of the Beechey Lake-Duggan Lake map area, District of Mackenzie, Northwest Territories; in Current Research, Part A, Geological Survey of Canada, Paper 82-1A, pp. 203-211.

Ghandi, S.S.

- 1985: Geology of the Artillery Pb-Zn-Cu district, Northwest Territories; in Current Research, Part A, Geological Survey of Canada, Paper 85-1A, pp. 359-363.

Gibb, R.A. and Thomas, M.D.

- 1977: The Thelon Front: A cryptic signature in the Canadian Shield?, Tectonophysics, 38, pp. 211-222.

Grotzinger, J.P. and Gall, Q.

- 1986: Preliminary investigations of Early Proterozoic Western River and Burnside River Formations: evidence for deep origin of Kilohigok Basin, District of Mackenzie; in Current Research, Part A, Geological Survey of Canada, Paper 86-1B, pp. 811-826.

Hanmer, S.

- 1984: The potential use of planar and elliptical structures as indicators of strain regime and kinematics of tectonic flow; in Current Research, Part B, Geological Survey of Canada, Paper 84-1B, pp. 133-142.

- 1986: Asymmetrical pull-aparts and foliation fish as kinematic indicators. J. Struct. Geol., 8, pp. 11-122.

Hanmer, S. and Connelly, J.N.

- 1986: Mechanical role of the syntectonic LaLoche Batholith in the Great Slave Lake Shear Zone, District of Mackenzie, N.W.T.; in Current Research, Part B, Geological Survey of Canada, Paper 86-1B, pp. 811-826.

Hanmer, S. and Lucas, S.B.

- 1985: Anatomy of a ductile transcurrent shear: the Great Slave Lake Shear Zone, District of Mackenzie, Northwest Territories (preliminary report); in Current Research; Part B, Geological Survey of Canada, Paper 75-1A, pp. 325-330.



- Henderson, J.B.  
1985: Geology of the Yellowknife-Hearne Lake area, District of Mackenzie: a segment across an Archean basin; Geological Survey of Canada, Memoir 414, 135p.
- Henderson, J.B. and McFie, R.I.  
1986: Artillery Lake map area, District of Mackenzie; a transect across the Thelon Front; in Current Research, Part A, Geological Survey of Canada, Paper 86-1A, pp. 411-416.
- Henderson, J.B., McGrath, P.H., James, D.T., McFie, R.I.  
1987: An integrated geological, gravity and magnetic study of the Artillery Lake area and the Thelon Tectonic Zone, District of Mackenzie; in Current Research, Part A, Geological Survey of Canada, Paper 87-1A, pp. 803-814.
- Henderson, J.B. and Thompson, P.H.  
1980: The Healey Lake map area (northern part) and the enigmatic Thelon Front, District of Mackenzie; in Current Research, Part A, Geological Survey of Canada, Paper 80-1A, pp. 165-169.  
  
1982: The Healey Lake map area and the Thelon Front problem, District of Mackenzie; in Current Research, Part A, Geological Survey of Canada, Paper 82-1A, pp. 191-195.
- Henderson, J.B., Thompson, P.H., and James, D.T.  
1982: The Healey Lake map area and the Thelon Front Problem, District of Mackenzie; in Current Research, Part A, Geological Survey of Canada, Paper 82-1A, pp. 191-195.
- James, D.T.  
1985: Geology of the Moraine Lake area and the Thelon Front, District of Mackenzie; in Current Research, Part A, Geological Survey of Canada, Paper 85-1a, pp. 449-454.  
  
1986: Geology of the Moraine Lake area, District of Mackenzie: a transect across the Thelon Tectonic Zone; in Current Research, Part A, Geological Survey of Canada, Paper 87-1A, report 71.
- Lister, G.S. and Price, G.P.  
1978: Fabric development in a quartz-feldspar mylonite, Tectonophysics, 49, pp. 37-78.

- Lister, G.S. and Snoke, A.W.  
1984: S-C Mylonites, J. Struct. Geol., 6, pp. 617-638.
- Lister, G.S. and Williams, P.F.  
1979: Fabric development in shear zones: theoretical controls and observed phenomena. J. Struct. Geol., 1, pp. 283-297.
- McFie, R.I.  
1987: The Clinton-Colden hornblende gabbro-anorthosite intrusion, Artillery Lake map area, District of Mackenzie; in Current Research, Part A, Geological Survey of Canada, Paper 87-1A, report 71.
- McGrath, P.H. and Henderson, J.B.  
1985: Reconnaissance ground magnetic and VLF profile data in the vicinity of the Thelon Front, Artillery Lake map area, District of Mackenzie; in Current Research, Part A, Geological Survey of Canada, Paper 85-1A, pp. 455-462.
- O'Donnell, L.L.  
1986: Characterization of the nature of deformation and metamorphic gradient across the Grenville Front Tectonic Zone in Carlyle Township, Ontario. Unpublished M.Sc. thesis, McMaster Univ., Hamilton, Ont.
- Passchier, C.W. and Simpson, C.  
1986: Porphyroclast systems as kinematic indicators, J. Struct. Geol., 8, pp. 831-843.
- Platt, J.P. and Vissers, R.L.M.  
1980: Extensional structures in anisotropic rocks, J. Struct. Geol., 2, pp. 397-410.
- Poirier, J.P. and Nicolas, A.  
1975: Deformation-induced recrystallization by progressive misorientation of subgrain-boundaries, with special references to mantle peridotites, Journal of Geology, 83, pp. 707-720.
- Ramsay, J.G. and Graham, R.H.  
1970: Strain variation in shear belts, Canadian Journal of Earth Sciences, 7, pp. 786-813.
- Ramsay, J.G. and Huber, M.I.  
1983: The Techniques of Modern Structural Geology. Volume 1: Strain Analysis. Academic Press. 307p.



- Simpson, C.  
 1983: Strain shape-fabric variations associated with ductile shear zones. J. Struct. Geol., 5, pp. 61-73.
- 1986: Determination of Movement Sense in Mylonites, Journal of Geological Education, 34, pp. 246-261.
- Simpson, C. and Schmid, S.M.  
 1983: An evaluation of criteria to deduce the sense of movement in sheared rocks, Geological Society of America Bulletin, 94, pp. 1281-1288.
- Stauffer, M.R.  
 1970: Deformation textures in tectonites, Canadian Journal of Earth Sciences, 7, pp. 498-511.
- Thomas, M.D., Gibb, R.A. and Quince, J.R.  
 1976: New evidence for offset aeromagnetic anomalies or transcurrent faulting associated with the Bathurst and McDonald faults, Northwest Territories; Canadian Journal of Earth Sciences, 13, pp. 1244-1250.
- Thompson, P.H., Culshaw, N., Buchannan, J.R., and Manojlovic, P.  
 1986: Geology of the Slave Province and Thelon Tectonic Zone in the Tinney Hills-Overby Lake (west half) map area, District of Mackenzie; in Current Research, Part A, Geological Survey of Canada, Paper 85-1A, pp. 407-420.
- Turner, F.J. and Weiss, L.E.  
 1963: Structural Analysis of Metamorphic Tectonites, McGraw-Hill Book Co. Inc., Toronto. QE 601.T94
- Urai, J.L., Means, W.D. and Lister, G.S.  
 1985: Dynamic recrystallization of minerals, American Geophysical Union Monograph, "in press", pp. 1-87.
- van Breeman, O., Henderson, J.B., Loveridge, W.D., and Thompson, P.H.  
 1987: U-Pb zircon and monazite geochronology and zircon morphology of granulites and granite from the Thelon Tectonic Zone, Healey Lake and Artillery Lake map areas, N.W.T., in Current Research, Part A, Geological Survey of Canada, Paper 87-1A, report 83.

- Vauchez, A., Miallet, D. and Songy, J.  
1987: Strain and deformation mechanisms in the Variscan nappes of Vendee, South Brittany, France, J. Struct. Geol., 9, pp. 31-40.
- Wakefield, J.  
1977: Mylonitization in the Lethakane shear zone, Journal of the Geological Society of London, 133, pp. 262-275.
- White, S.H.  
1975: Tectonic deformation and recrystallization of oligoclase, Contributions to Mineralogy and Petrology, 50, pp. 287-304.  
1976: The effects of strain on the microstructure, fabrics and deformation mechanisms in quartz; Philosophical Transactions of the Royal Society of London, Series A, 283, pp. 69-86.
- White, S.H., Burrows, S.E., Carreras, J., Shaw, N.D. and Humphreys, F.J.  
1980: On mylonites in ductile shear zones, J. Struct. Geol., 2, pp. 175-187.
- White, S.H., Evans, D.J., and Zhang, D.L.  
1982: Fault rocks of the Moine thrust zone; microstructures and textures of selected mylonites. Textures and Microstructures, 5, pp. 33-61.
- Winkler, H.G.F.  
1979: Petrogenesis of Metamorphic Rocks, 5th ed., Springer-Verlag, 348p.
- Wright, G.M.  
1957: Geological Notes on eastern District of Mackenzie, Northwest Territories; Geological Survey of Canada, Paper 56-10.  
1967: Geology of the southeastern barren grounds, parts of the District of Mackenzie and District of Keewatin (Operations Keewatin, Baker and Thelon); Geological Survey of Canada, Memoir 350, 91p.



